Maintenance of critical industrial equipment using cosmic muon radiation.

Pablo Martínez Ruiz del Árbol

27th May 2019
University of Zürich

Outline of the talk

- Cosmic muons: numbers, orders of magnitude and detectors.
- Muography: Principles, types, applications.
- Maintenance of industrial equipment using muography: Muon Systems.
- The future of Muography and next steps.

Cosmic rays: composition, flux, energy spectrum.

Cosmic rays: composition, flux, energy spectrum.

- Constant flux of high energy particles bombarding the Earth from the space.
- Composed mainly by protons (98%), α particles (1.8%) and others (< 0.2%)
- Cosmic rays are the most energetic particle ever seen so far.

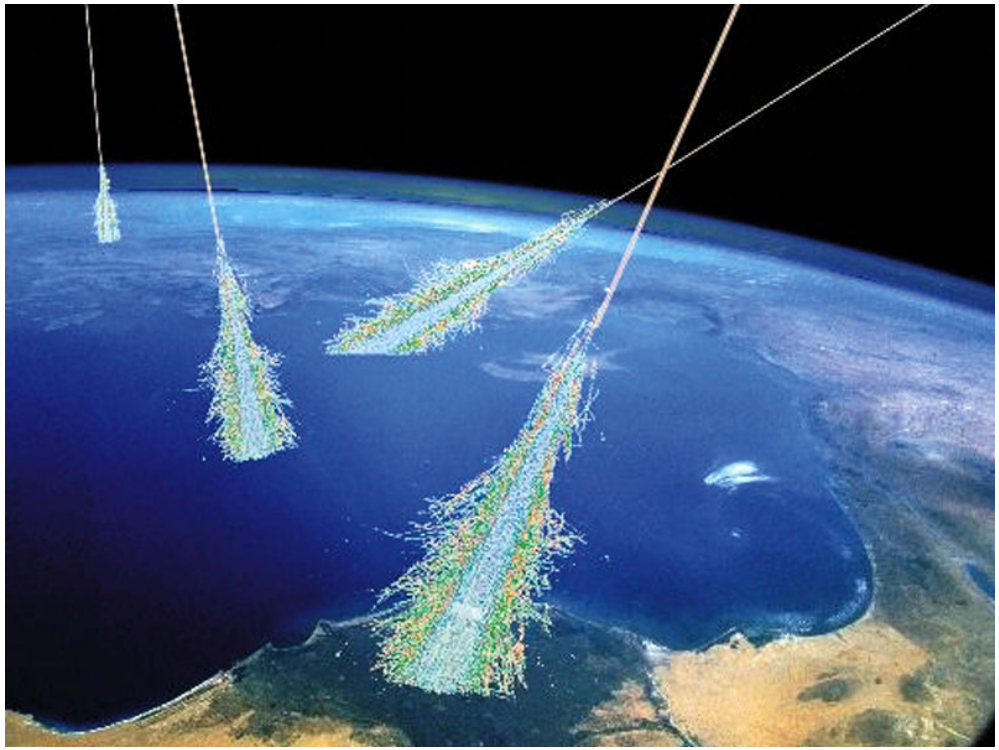

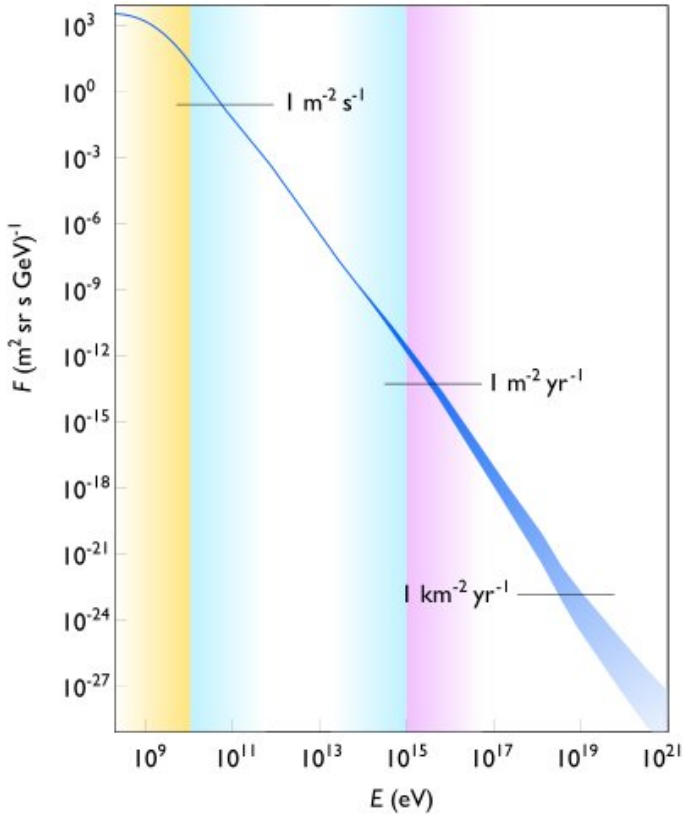

The Oh-My-God Particle 3x10^{8} TeV (1991, several since then) → http://www.cosmic-ray.org/reading/flyseye.html#SEC10

Cosmic muons: flux and energy spectrum.

- Muons are generated mostly from pion decays in the atmosphere.
- The flux of muons is mostly proportional to $\cos^2(\theta)$ (angle with the vertical).
- Quickly falling spectra → average of **3 GeV** when integrating solid angle.

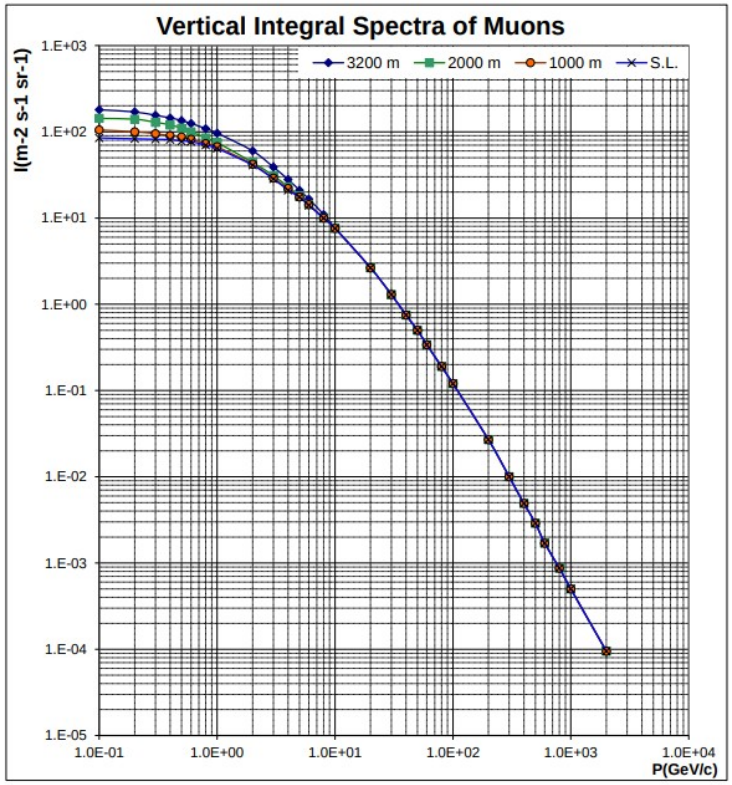

Rule of thumb at the surface:

10000 muons per squared meter and minute.

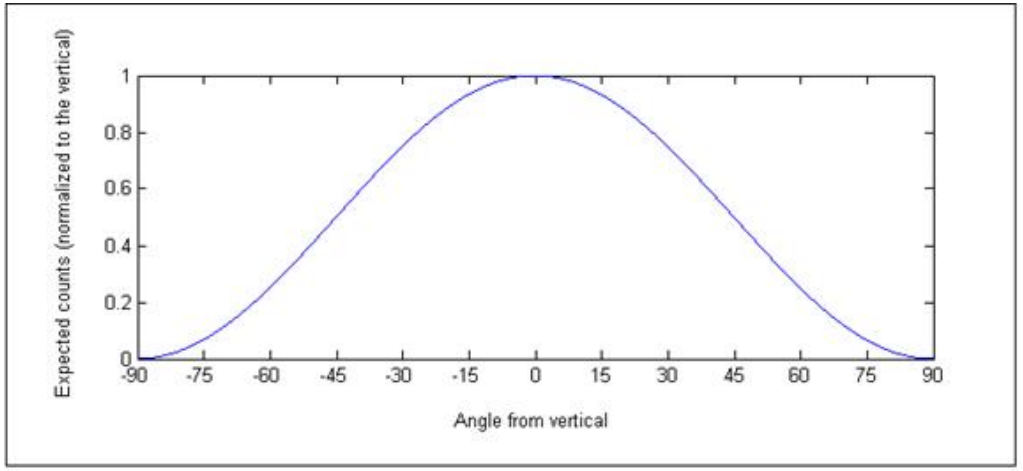

Muon interaction with matter: ionization.

- Ionization is one of the most frequent processes for cosmic muons.
- Energy loss depends on the Z, density, and size of the crossed object.
- The Range is the distance for which the particle looses all the energy.

$$-\left\langle \frac{dE}{dx} \right\rangle = \frac{4\pi}{m_e c^2} \cdot \frac{n z^2}{\beta^2} \cdot \left(\frac{e^2}{4\pi\varepsilon_0} \right)^2 \cdot \left[\ln\left(\frac{2 m_e c^2 \beta^2}{I \cdot (1-\beta^2)} \right) - \beta^2 \right]$$

Mean excitation potential

$$n = \frac{N_A \cdot Z \cdot \rho}{A \cdot M_u}$$

Muon Energy/GeV	Material	Range/m
1	Water	471
10	Water	4260
1	Concrete	228
10	Concrete	2025
1	Standard Rock	209
10	Standard Rock	1857

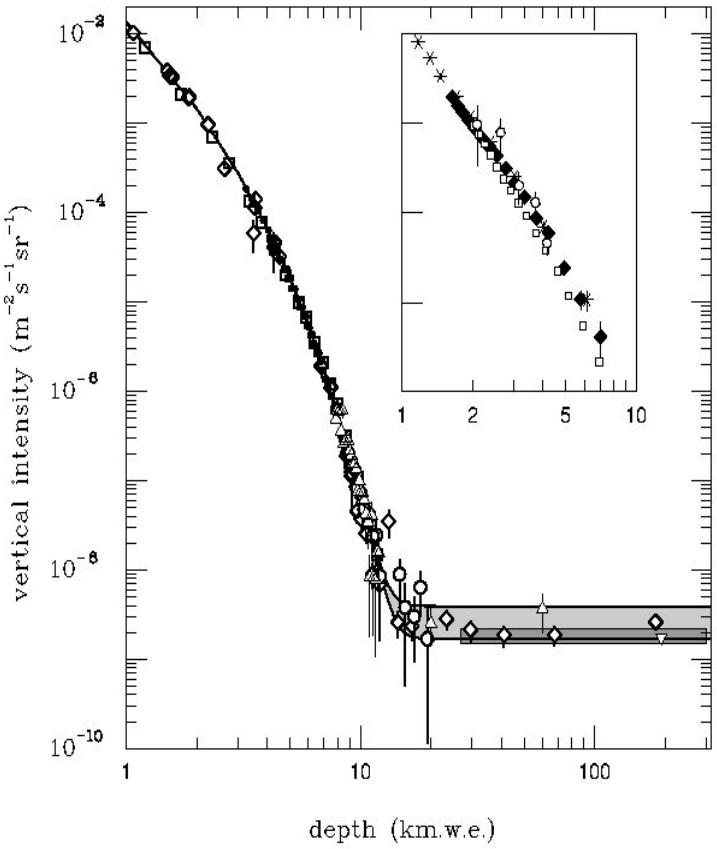

Muons interaction with matter: multiple scattering.

- Coulomb scattering deviates the direction of muons when crossing matter.
- Scattering angle depends also on the Z, density, and size of the material.
- Angular distribution is approximately gaussian (with some tails).

Momentum dependence

$$\theta_0 = \frac{13.6}{\beta cp} z\sqrt{x/X_0}\,[1 + 0.038 \ln(x/X_0)]$$

$$X_0 = 716.4\ \mathrm{g\,cm^{-2}} \frac{A}{Z(Z+1)\ln\frac{287}{\sqrt{Z}}}$$

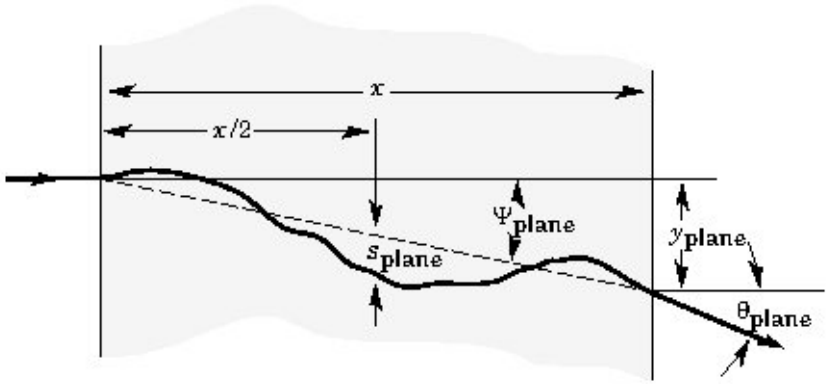

Muon Energy/GeV	Material	Width/cm	Angle/mrad
1	Iron	1	10
10	Iron	1	1
1	Iron	10	34
10	Iron	10	3
1	Lead	1	19
10	Lead	1	2
1	Lead	10	64
10	Lead	10	6
1	Uranium	1	26
10	Uranium	1	3
1	Uranium	10	88
10	Uranium	10	9

Muon detectors using different technologies.

- Multiwire proportional chambers and drift tubes (gaseous detectors).
- Scintillitator detectors (of different kinds) + photomultipliers.
- Sillicon-based detectors: pixel-like, strip-like, etc.
- Important parameters: spatial resolution (granularity), efficiency, acceptance.

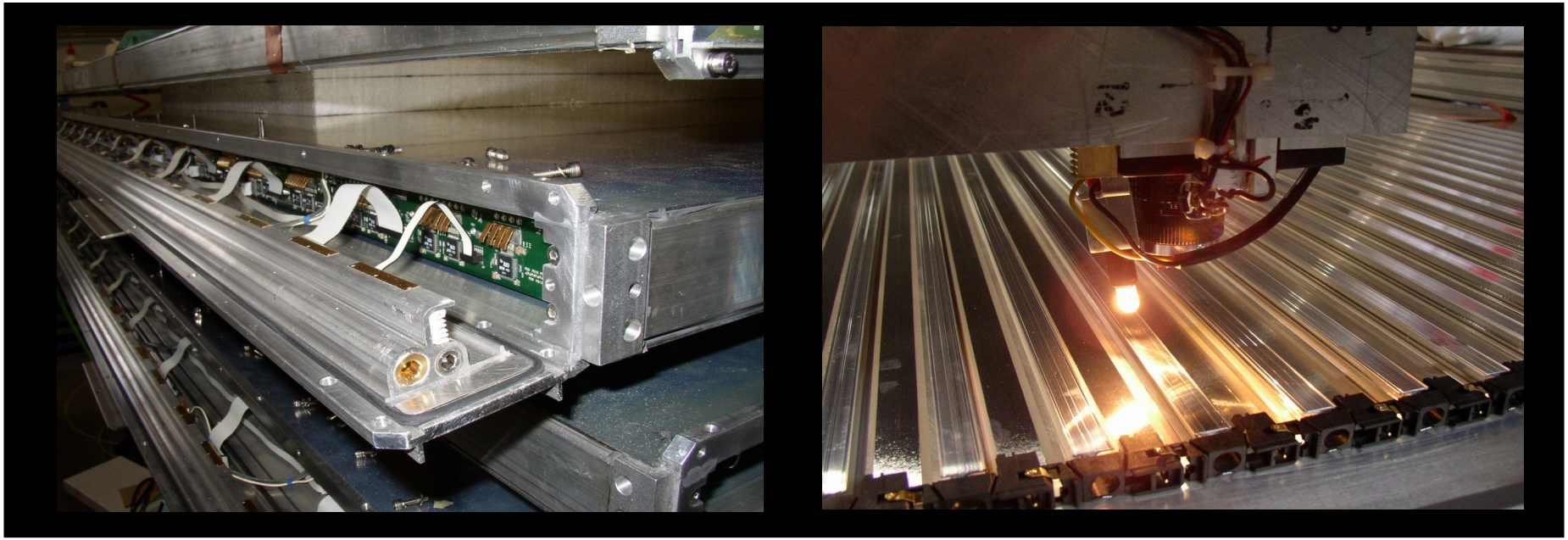

http://cds.cern.ch/record/942973 → CIEMAT assembly of DT chambers

Muography: principles, types, and applications.

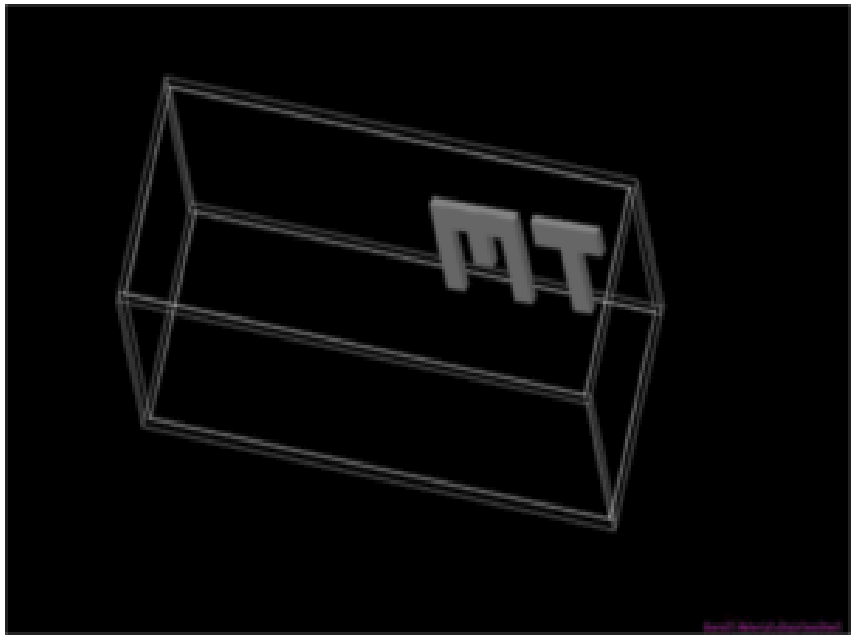

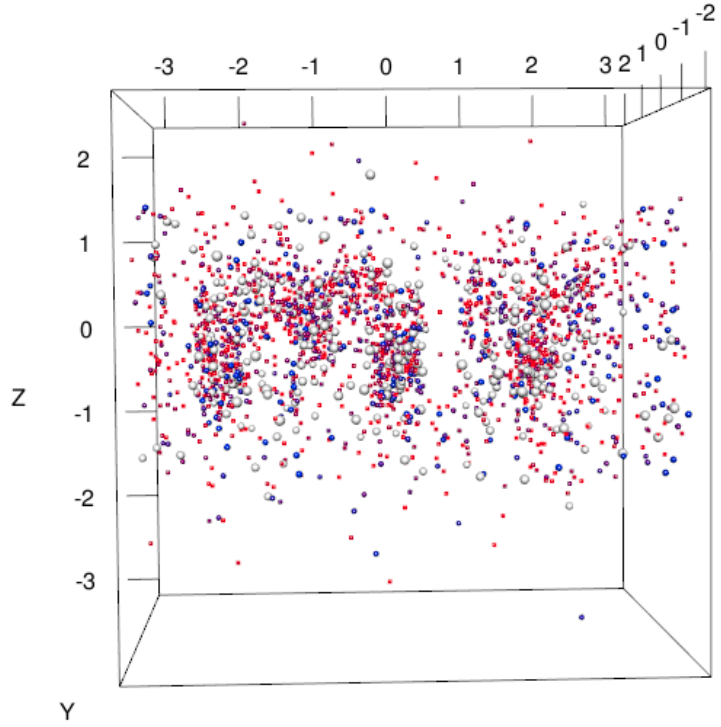

An old (documented) Muography application.

- Muography uses cosmic muons to obtain images of unaccesible places.
- First attempt by Luis Álvarez in 1970 to find hidden chambers in pyramids.

Search for Hidden Chambers in the Pyramids

The structure of the Second Pyramid of Giza is determined by cosmic-ray absorption.

Luis W. Alvarez, Jared A. Anderson, F. El Bedwei, James Burkhard, Ahmed Fakhry, Adib Girgis, Amr Goneid, Fikhry Hassan, Dennis Iverson, Gerald Lynch, Zenab Miligy, Ali Hilmy Moussa, Mohammed-Sharkawi, Lauren Yazolino

The three pyramids of Giza are situated a few miles southwest of Cairo, Egypt. The two largest pyramids stand within a few hundred meters of each other. They were originally of almost exactly the same height (145 meters), but the Great Pyramid of Cheops has a slightly larger square base (230 meters on a side) than the Second Pyramid of Chephren (215.5 meters on a side). A photograph of the pyramids at Giza is shown as Fig. 1. Figure 2 shows the elevation cross sections of the two pyramids and indicates the contrast in architectural design. The simplicity of Chephren's pyramid, compared with the elaborate structure of his father's Great Pyramid, is explained by archeologists in terms of a "period of experimentation," ending with the construction of Cheops's pyramid (*1*). (The complexity of the internal architecture of the pyramids increased during the Fourth Dynasty until the time of Cheops and then gave way to quite simple designs after his time.)

An alternative explanation for the sudden decrease in internal complexity from the Great Pyramid to the Second Pyramid suggested itself to us: perhaps Chephren's architects had been more successful in hiding their upper chambers than were Cheops's. The interior of the Great Pyramid was reached by the tunneling laborers of Caliph Mamun in the 9th century A.D., almost 3400 years after its construction. Of our group only Ahmed Fakhry (author of *The Pyramids*, professor emeritus of archeology, University of Cairo, and member of the Supreme Council of Archeology, Cairo) was trained in archeology. As laymen, we thought it not unlikely that unknown chambers might still be present in the limestone above the "Belzoni Chamber," which is near the center of the base of Chephren's Second Pyramid, and that these chambers had survived undetected for 4500 years. [We learned later that such ideas had occurred to early 19th-century investigators (*2*), who blasted holes in the pyramids with gunpowder in attempts to locate new chambers.]

In 1965 a proposal to probe the Second Pyramid with cosmic rays (*3*) was sent to a representative group of cosmic-ray physicists and archeologists with a request for comments concerning its technical feasibility and archeological interest. The principal novelty of the proposed cosmic-ray detectors involved their ability to measure the angles of arrival of penetrating cosmic-ray muons with great precision, over a large sensitive area. The properties of the penetrating cosmic rays have been sufficiently well known for 30 years to suggest their use in a pyramid-probing experiment, but it was not until the invention of spark chambers with digital read-out features (*4*) that such a use could be considered as a real possibility. [Cosmic-ray detectors with low angular resolution had been used in 1955 to give an independent measure of the thickness of rock overlying an underground powerhouse in Australia's Snowy Mountains Scheme (*5*)].

The favorable response to the proposal led to the establishment by the United Arab Republic and the United States of America of the Joint U.A.R.–U.S.A. Pyramid Project on 14 June 1966. Cosmic-ray detectors were installed in the Belzoni Chamber of the Second Pyramid at Giza in the spring of 1967 by physicists from the Ein Shams University and the University of California, in cooperation with archeologists from the U.A.R. Department of Antiquities. Initial operation had been scheduled for the middle of June 1967, but for reasons beyond our control the schedule was delayed for several months. In early 1968 cosmic-ray data began to be recorded on magnetic tape in our laboratory building, a few hundred meters from the two largest pyramids. Since that time we have accumulated accurate angular measurements on more than a million cosmic-ray muons that have penetrated an average of about 100 meters of limestone on their way to the detectors in the Belzoni Chamber.

Proof of the Method

Before any new technique is used in an exploratory mode, it is essential that the capabilities of the technique be demonstrated on a known system. We gave serious consideration to a proposal that the cosmic-ray detectors be tested first in the Queen's Chamber of the Great Pyramid, to demonstrate that the King's Chamber and the Grand Gallery could be detected. But this suggestion was abandoned because the King's Chamber is so close to the Queen's Chamber and because it subtends such a large solid angle that earlier (low resolution) cosmic-ray experiments had already shown that the upper chamber would give a large signal. It was apparent that the only untested feature of the new technique involved the magnitude of the scattering of high energy muons in solid matter. (An anomalously large scattering would nullify the high angular resolution that had been built into the detectors, in the same way that frosted glass destroys our ability to see distant objects.) We had no reason to doubt the calculated scattering, but we were anxious to be able to demonstrate to our colleagues in the U.A.R. Department of Antiquities in a convincing manner that the technique really worked as we had calculated. For this purpose we required as our test objects not large features that were nearby but, instead, small features separated from the detectors by the greatest possible thickness of limestone. Fortunately, such features are available in the Second Pyramid; the four diagonal ridges that mark the intersections of neighboring plane faces were farther from the detectors than any other points on the individual faces. (From now on, we will refer to these ridges as the "corners.")

From the known geometry of the Second Pyramid, the trajectories of cosmic-ray muons that pass through a point on a face 10 meters from a corner and then down to the detectors can be shown to traverse 2.3 fewer meters of limestone than do muons that strike the corner. They should therefore arrive with 5 percent greater intensity than the muons from the corner. Such an increase in intensity, corresponding to such a decrease in path through the limestone, is about half of what would be expected to result from the presence of a chamber of "typical size" (5 meters high) in the pyramid. Since such a chamber would necessarily be closer to the detectors, it would for these two reasons be a much "easier object to see" than the corner.

The detection equipment was therefore installed in the southeast corner of the Belzoni Chamber, with the expectation that it would first show the corners in a convincing manner, so that the presence or absence of unknown chambers could later be demonstrated to the satisfaction of all concerned. In September 1968 the IBM-1130 computer at the Ein Shams University Computing Center produced the data

832

The authors are affiliated with the Joint Pyramid Project of the United Arab Republic and the United States of America. They reside either in Cairo, United Arab Republic, or in Berkeley, California. The article is adapted from an address presented by Luis W. Alvarez at the Washington Meeting of the American Physical Society, 30 April 1969.

Fig. 1 (top right). The pyramids at Giza. From left to right, the Third Pyramid of Mycerinus, the Second Pyramid of Chephren, the Great Pyramid of Cheops. [© National Geographic Society]

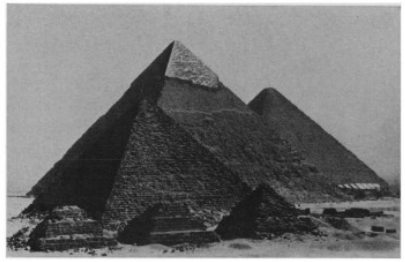

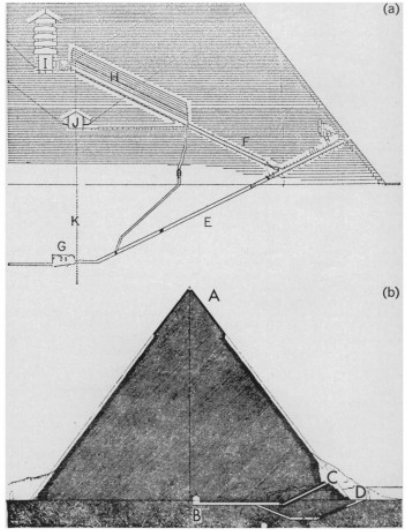

Fig. 2 (bottom right). Cross sections of (a) the Great Pyramid of Cheops and (b) the Pyramid of Chephren, showing the known chambers: (*A*) Smooth limestone cap, (*B*) the Belzoni Chamber, (*C*) Belzoni's entrance, (*D*) Howard-Vyse's entrance, (*E*) descending passageway, (*F*) ascending passageway, (*G*) underground chamber, (*H*) Grand Gallery, (*I*) King's Chamber, (*J*) Queen's Chamber, (*K*) center line of the pyramid.

"We have no doubt that we could detect a King's Chamber anywhere above the Belzoni Chamber within a cone of half-angle 35 degrees from the vertical.

If the Second Pyramid architects had placed a Grand Gallery, King's Chamber, and Queen's Chamber in the same location as they did in Cheops's Pyramid, the signals from each of these three cavities would have been enormous.

We therefore conclude that no chambers of the size seen in the four large pyramids of the Fourth Dynasty are in our "field of view" above the Belzoni Chamber."

http://lappweb.in2p3.fr/~chefdevi/Work_LAPP/Arche/alvarez_70.pdf

Two categories on muography applications.

- Two categories according to the physics process: absorption vs. scattering.

Absorption Muography

- Muon flux measured as a function of the direction.
- Differential transmittance “T”.
- Need Large Masses + Long exposure times.
- Applications: vulcanology, geology, archeology…
- Only one detector needed.

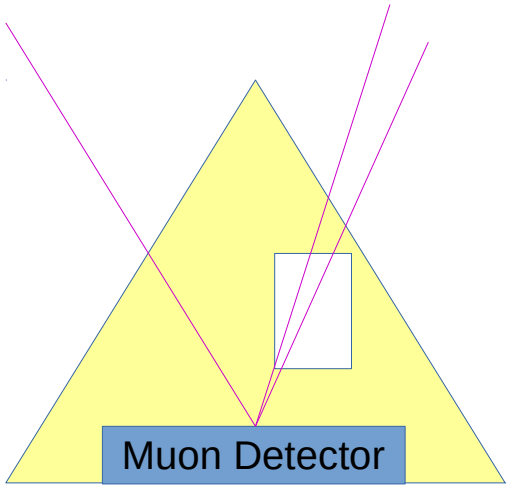

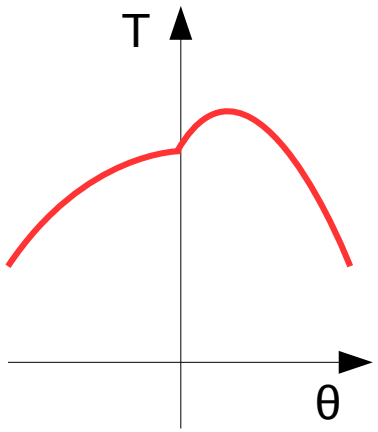

Scattering Muography

- Scattering position and angular shift.
- Smaller Masses + shorter exposure times.
- Applications: security, industry, etc.
- At least two detectors are needed.

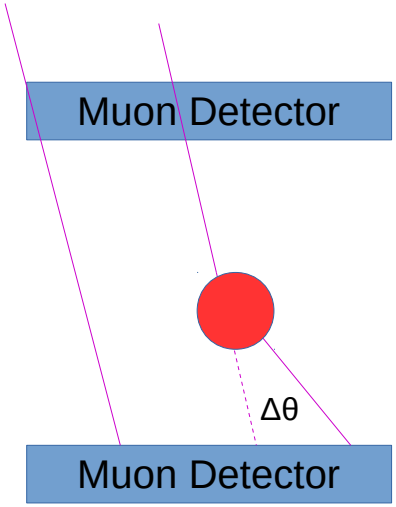

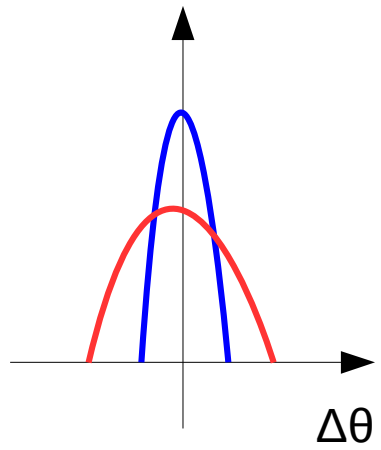

The inverse problem in muon tomography.

- Tomography is a classic “inverse problem” type of challenge.

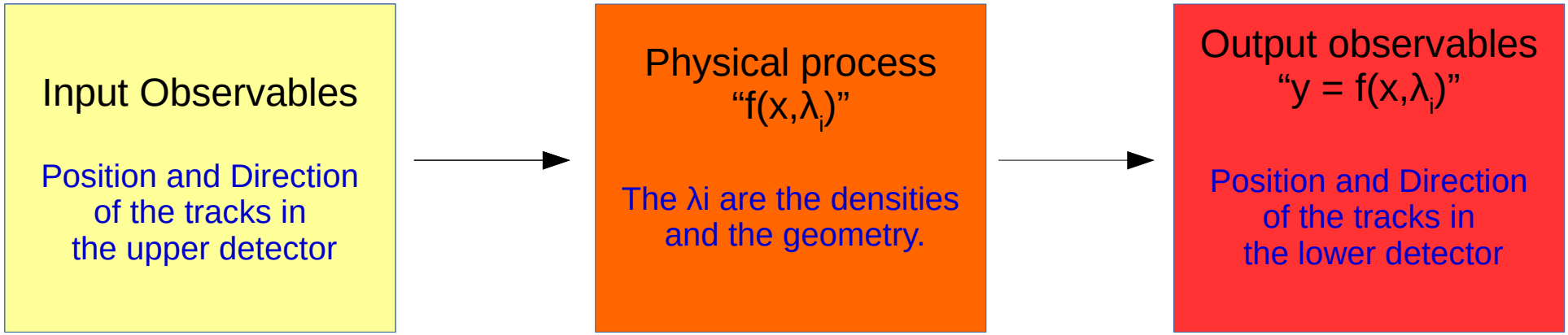

- Where the physical process depends on some parameters λi
- And where we know how to solve the **forward problem:**
  - Given “x” and “λ_i” we know how to estimate “y”.
- The inverse problem consists of estimating “λ_i” when having “x” and “y”
- **BUT: in this case f() is not a deterministic function → it is a probability density.**

The simple geometric approach: POCA

- This complex problem can be approximated doing some physical assumptions
  - The scattering occurs only at one point during the whole trajectory.
  - Works very well for scenarios that are essentially empty with some high density chunks.
- The scattering is assumed to be produced in the Point of Closest Approach.
- And the density is assumed to be in the places where there is scattering.

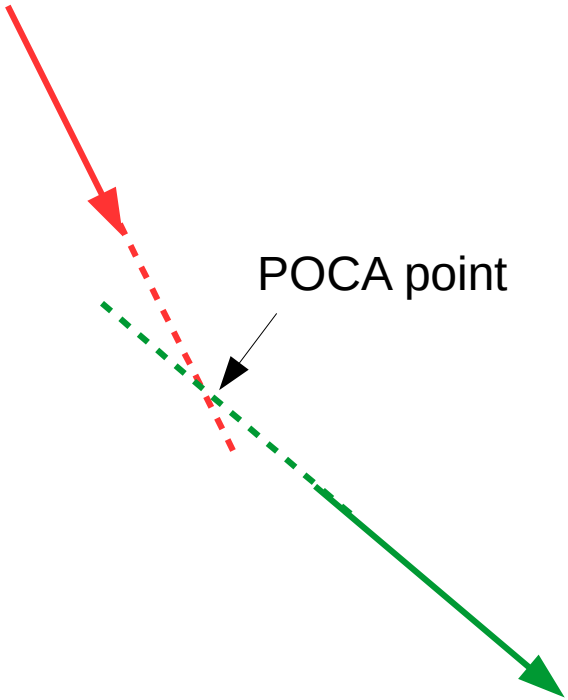

Point of **C**losest **A**pproach (POCA)

The “I wish” Maximum Likelihood solution

- Since the forward problem is known one could thing about applying Wick’s theorem
  - Fill the target volume with a set of voxels of random density.
  - For every input muon calculate the pdf of the output muon using simulation.
  - Evaluate the output muon in the pdf and accumulate in the likelihood function.
  - Minimize the likelihood to get the best densities.
- This is just impossible due to time/computing resources.

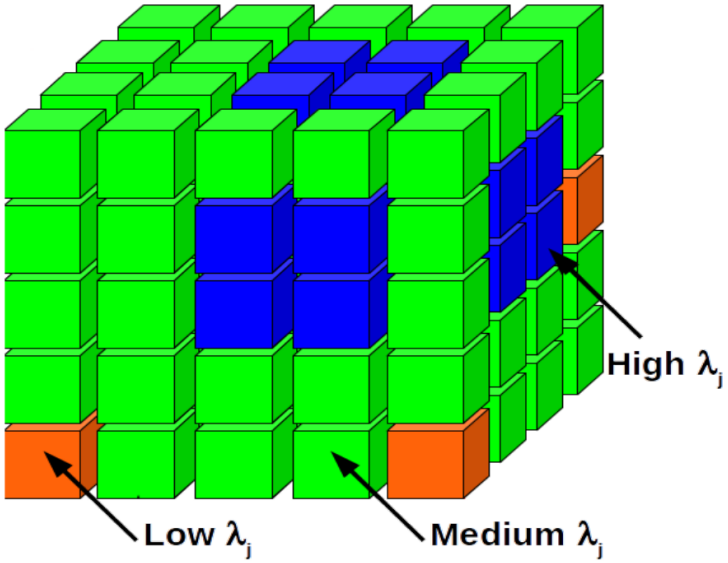

$$L(x, y; \lambda) = \prod pdf(y_i; x_i, \lambda)$$

$$min\, L(x, y; \lambda)$$

The “poor-man” Maximum Likelihood solution

- The complexity of the previous procedure reduces drastically if:
  - The propagation of the muon is approximated as a product of gaussians in the voxels.
  - The voxels crossed for each muon are fixed and approximated (under some assumption).
- Under this conditions an analytical likelihood can be obtained:

$$P(H_{ij}\,|\,\lambda) = \frac{1}{2\pi|\Sigma_{ij}|^{1/2}} \exp\left(-\frac{1}{2} H_{ij}^T \Sigma_{ij}^{-1} H_{ij}\right) \qquad \log(P(H\,|\,\lambda)) = \sum_{j\leq N} \sum_{i:L_{ij}\neq 0} \left(-\log\lambda_j - \frac{H_{ij}^T A_{ij}{}^{-1} H_{ij}}{2\lambda_j p_{r,i}^2}\right) + C \quad (34)$$

- However the procedure is also quite time expensive and
- The results are not dramatically better than POCA:
  - Since in the end a POCA assumption is made on the trajectory of the muons.

Application to vulcanology

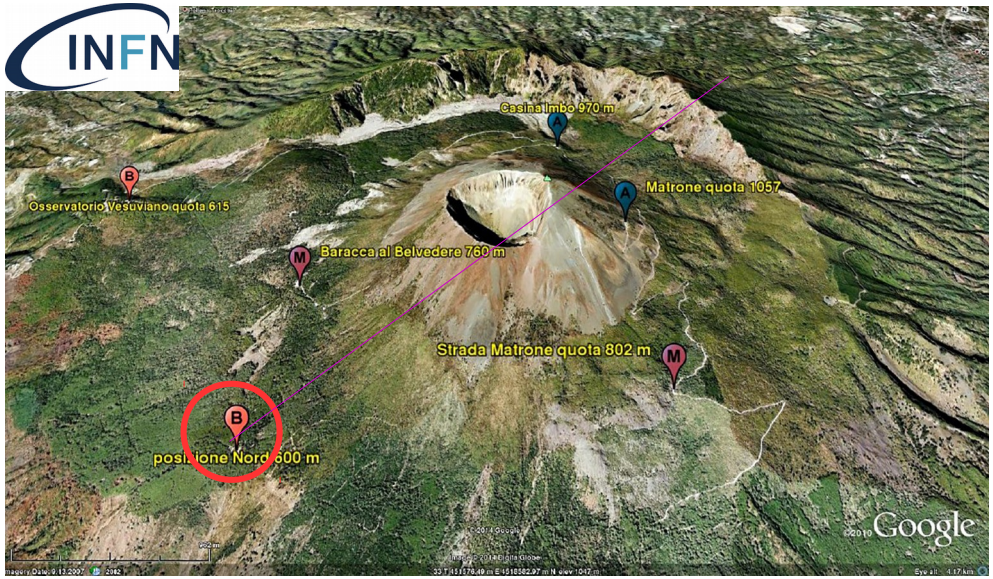

Monitoring of Vesuvious vulcano.

https://doi.org/10.1098/rsta.2018.0050

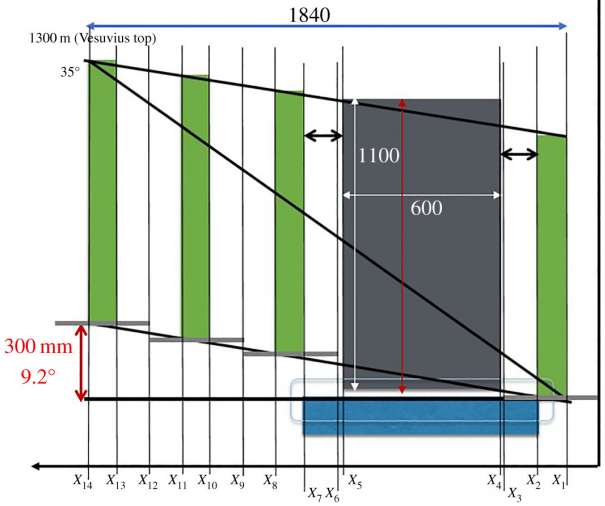

X_1	125	0
X_2	235	+110
X_3	360	+125
X_4	385	+25
X_5	985	+600
X_6	1010	+25
X_7	1135	+125
X_8	1245	+110
X_9	1370	+125
X_{10}	1495	+125
X_{11}	1605	+110
X_{12}	1730	+125
X_{13}	1855	+125
X_{14}	1965	+110

Only 1 scintillator detector.

Exposure time ~ year.

Dinamic studies on magma convenction.

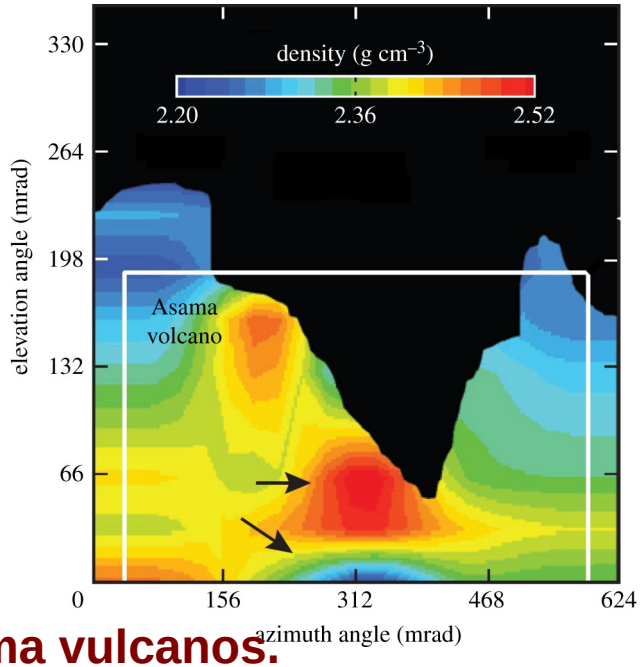

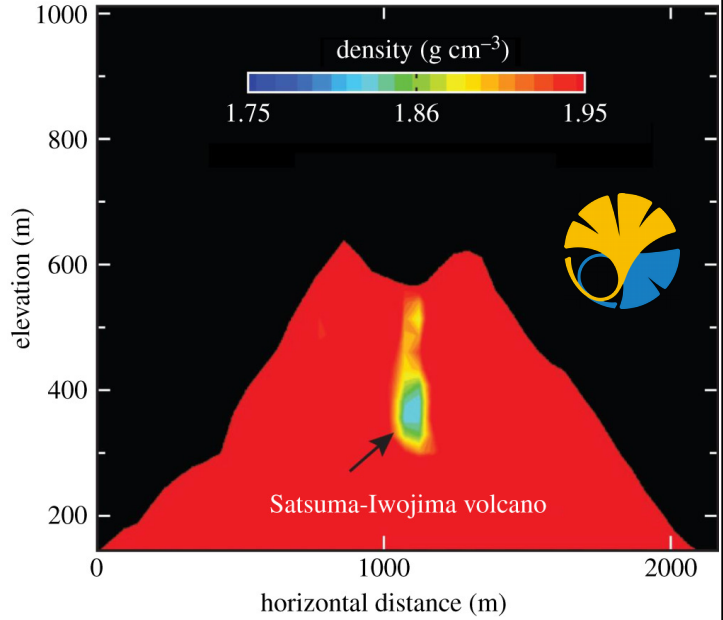

Monitoring of Asama & Iwujima vulcanos.

https://doi.org/10.1098/rsta.2018.0142

Application to mineral mines.

https://doi.org/10.1098/rsta.2018.0061

Search for uranium/lead clusters in McArthur River (Canada) and Pend Oreille (USA)

Canadian Private company:

CRM Geotomography Technologies, Inc.,

Grid of scintillator detectors in the galleries.

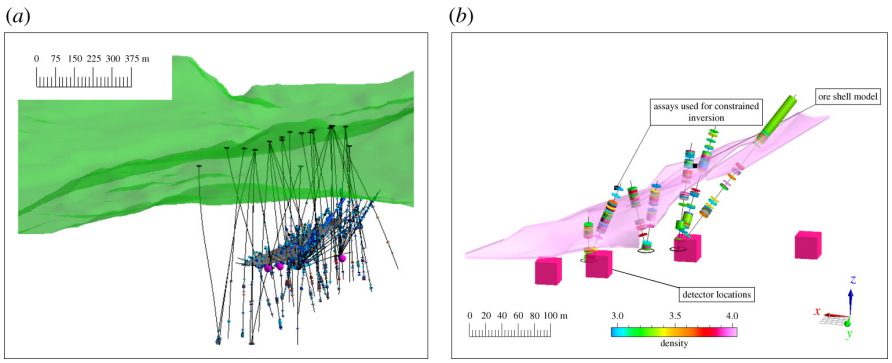

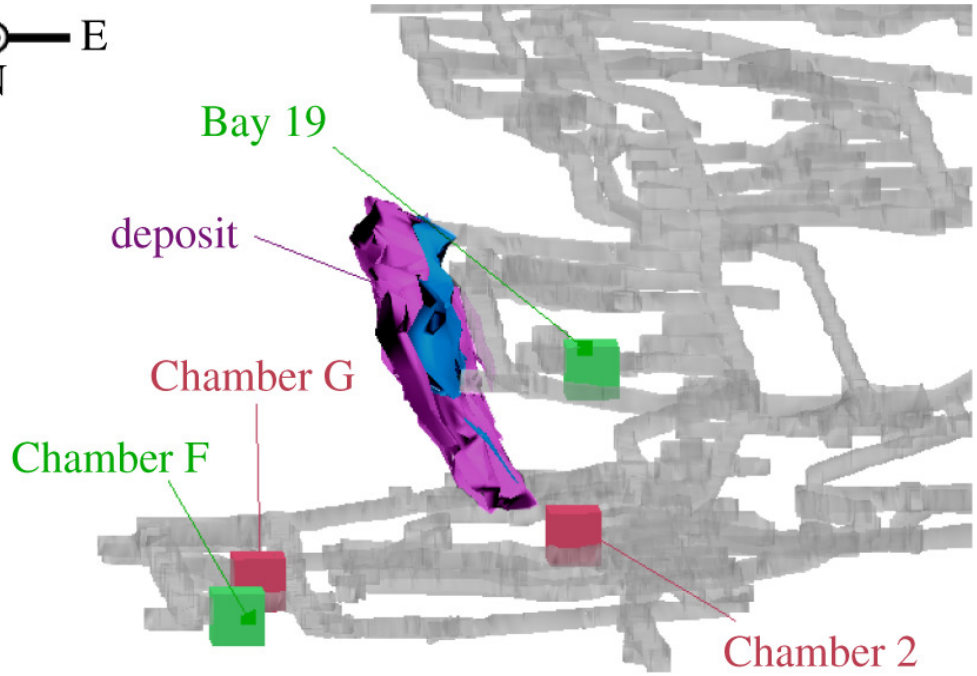

Underground mapping for pipe location.

https://doi.org/10.1098/rsta.2018.0133

Israel Private company:

Lingacom S.L,

Cylindrical-scintillator detectors.

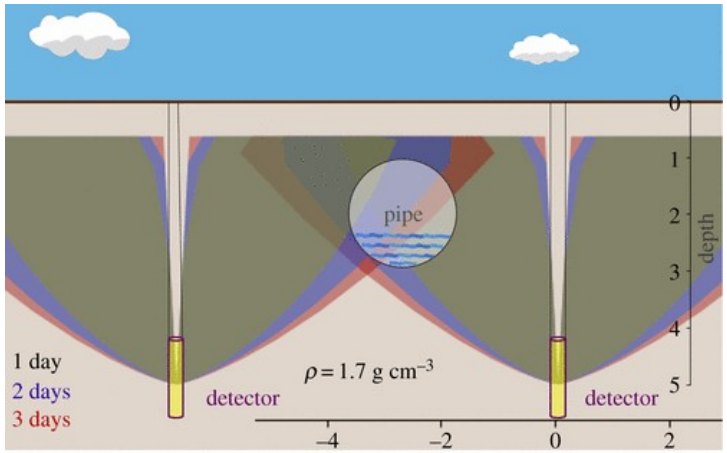

Application to archeology/civil engineering.

Search for hidden galleries in Mount Echia (Bourbon Tunnel)

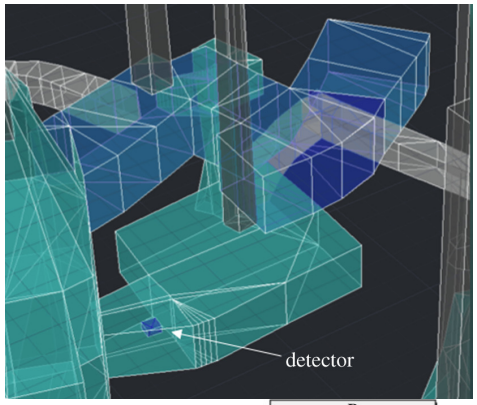

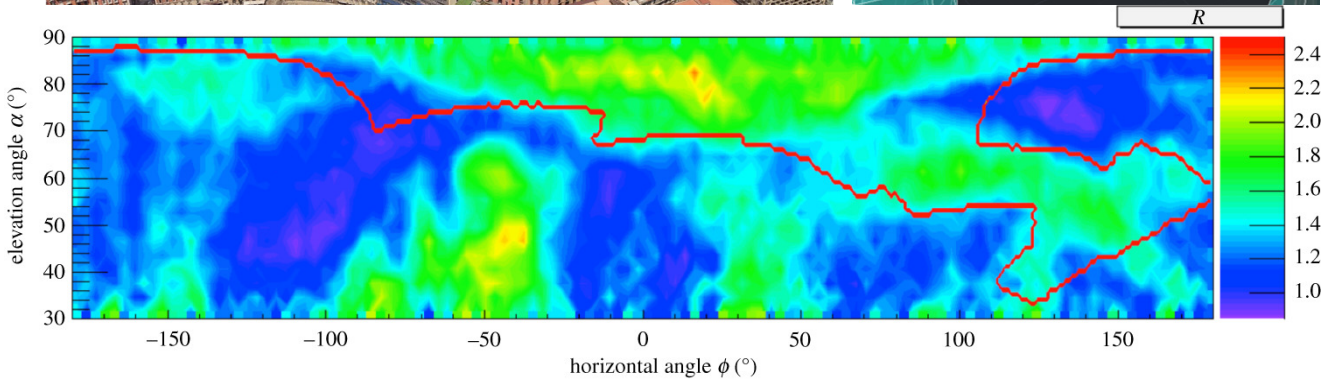

https://doi.org/10.1098/rsta.2018.0057

Only 1 scintillator detector.

Exposure time ~ 26 days.

Monitoring of the dome of Santa Maria del Fiore.

https://doi.org/10.1098/rsta.2018.0136

One of the only scattering-based applications in civil engineering.

Two drift tube chambers located outside and inside the dome.

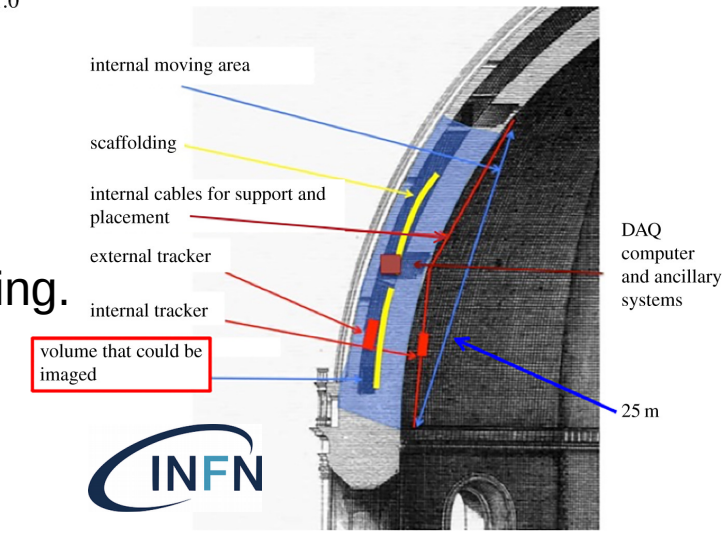

Application to border security.

Truck inspection using cosmic muons.

https://doi.org/10.1098/rsta.2018.0051

Using CMS-like chambers at Torino.

For this application: 4 chambers.

Detection of a 7cmx7cmx7cm lead box.

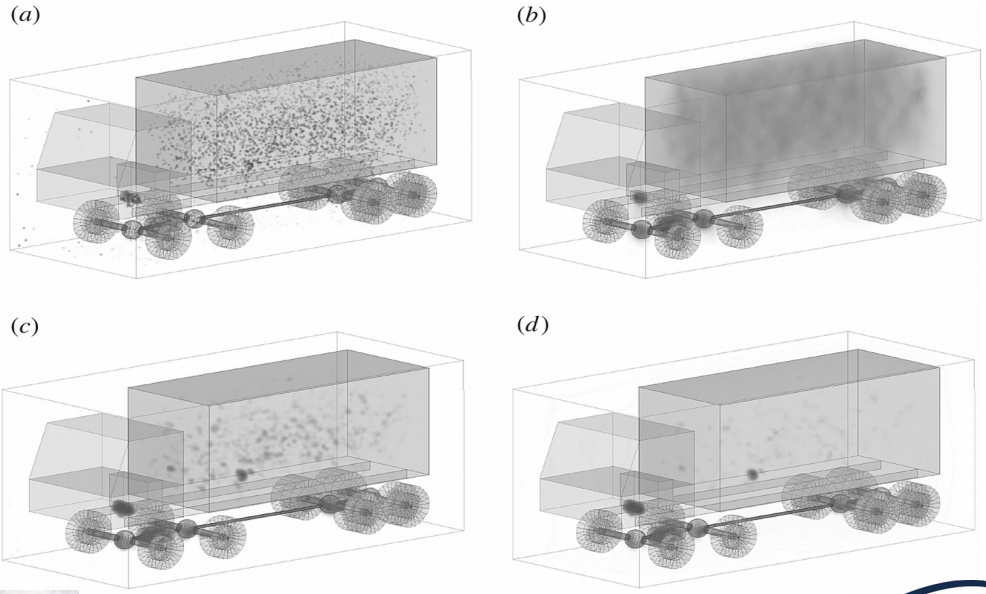

INFN

Decision Science

First commercial system.

First contract in Singapur to install portal.

Multi-technology detection portal.

https://decisionsciences.com/

Application to the nuclear industry.

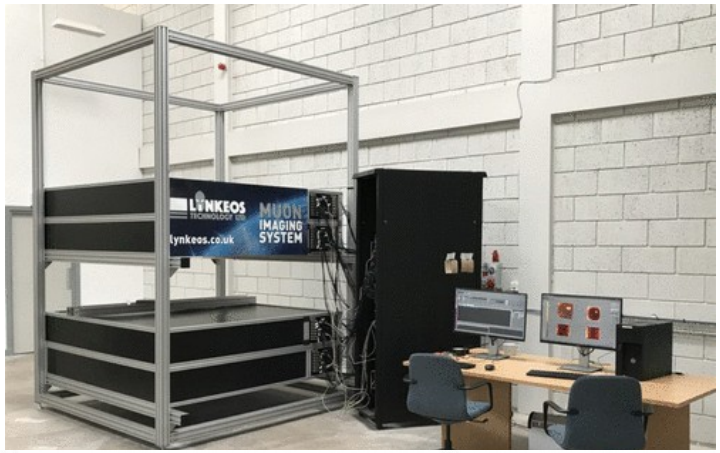

Nuclear waste characterization.

Lynkeos Technology Ltd (University of Glasgow)

UK Nuclear Decommissioning Authority.

Commercial Scintillator detector.

https://doi.org/10.1098/rsta.2018.0048

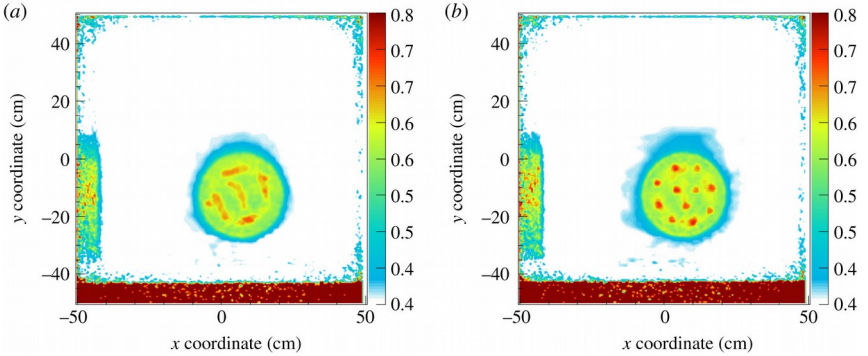

Exposure times of about 7 hours.

Effective detection of missing fuel.

Fuel cask monitoring.

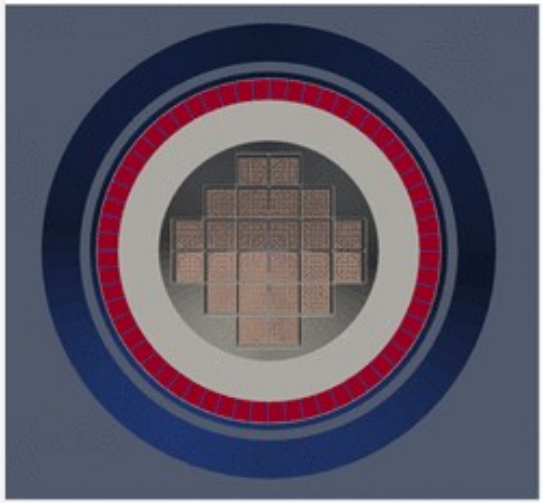

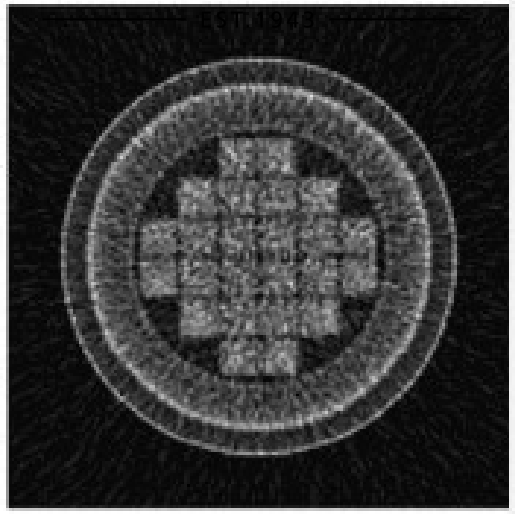

https://doi.org/10.1098/rsta.2018.0052

Maintenance of industrial equipment using Muography: Muon Systems

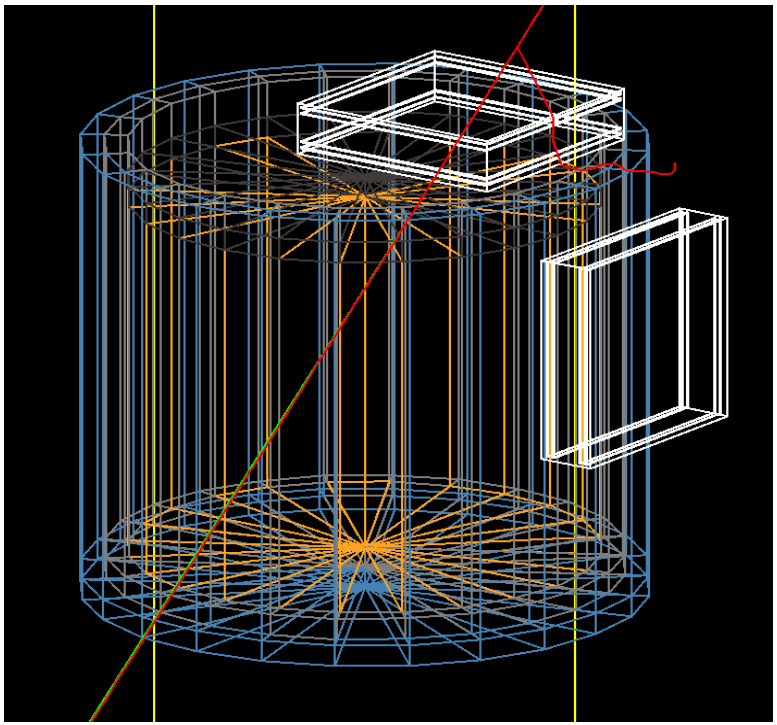

Degradation of the interior of industrial equipment.

Impact in the operation due to the changes in the width in critical parts of the installation: pipes, cauldrons, blast furnaces.

Humidity, corrosion, high pressure and temperature.

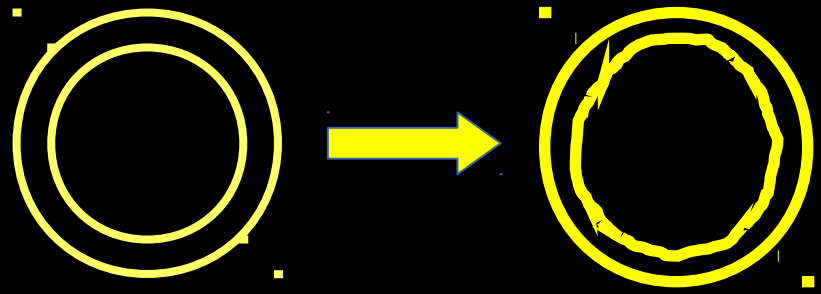

Changes in the width of the walls.
Alteration of mechanical conditions.

Preventive stops (blast furnaces).
Measurement of the width.

High economical and potentially energetic cost of unexpected stops.

Muon Systems: a young Muography company.

- Founded in 2017 by 2 members using private capital.
- Based on Bilbao (Edificio Ilgner, Altos Hornos de Vizcaya).
- Currently 3 employees + 1 consultant.

https://muon.systems/

New input in preventive maintenance.

- Using multiple scattering to reconstruct the inner geometry of the equipment.
  - High penetration power.
  - No physical contact with the facility.
  - No need of stopping the productive process.
  - Possibility to perform continuous monitoring for critical cases.

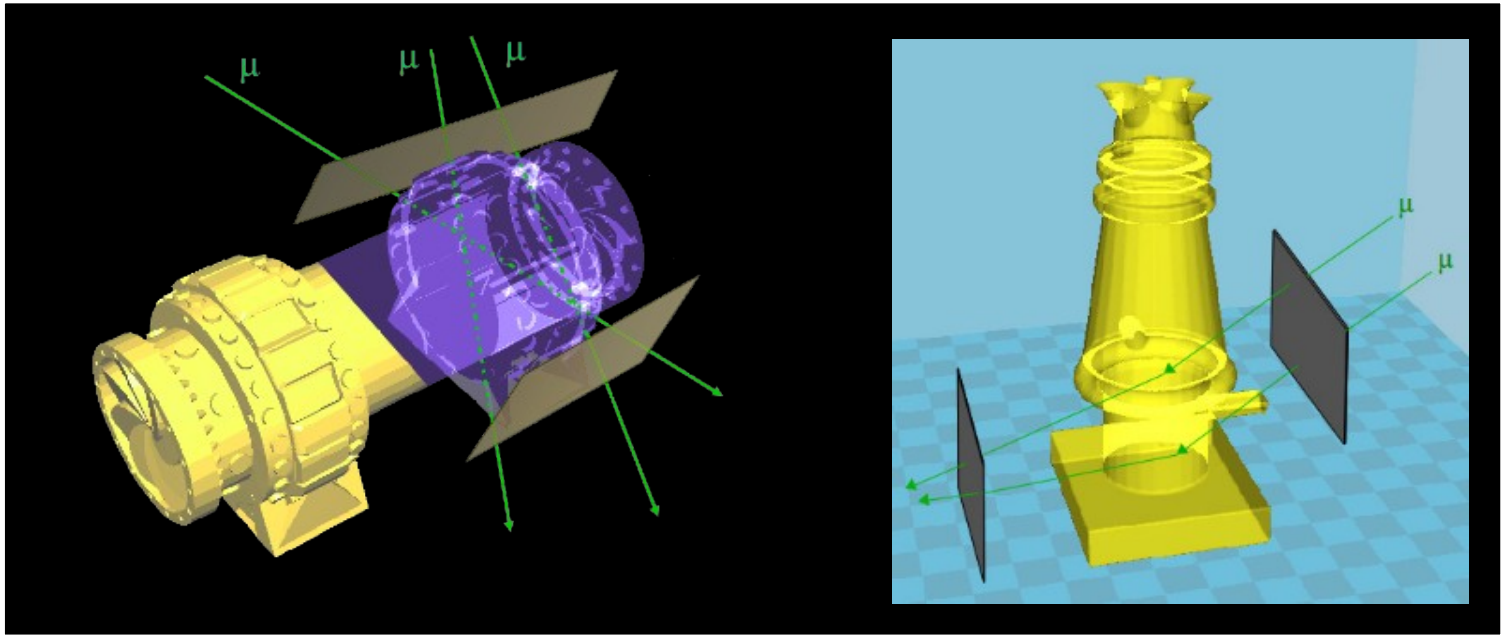

Financial/technical support from many institutions.

Area 1: Innovative projects.

Ekintzaile: Innovative projects.

Best national project in manufacturing and materials CDTI – NEOTEC 2017

Progress in control of processes and maintenance.

Accelerated by FDE.

Sidenor challenge.

A lot of interest from many different companies.

- Different problems ranging from huge facilities to small equipment.
- In this presentation I will be focusing on the problem of insulated pipes.

Measurement of the width of an insulated pipe.

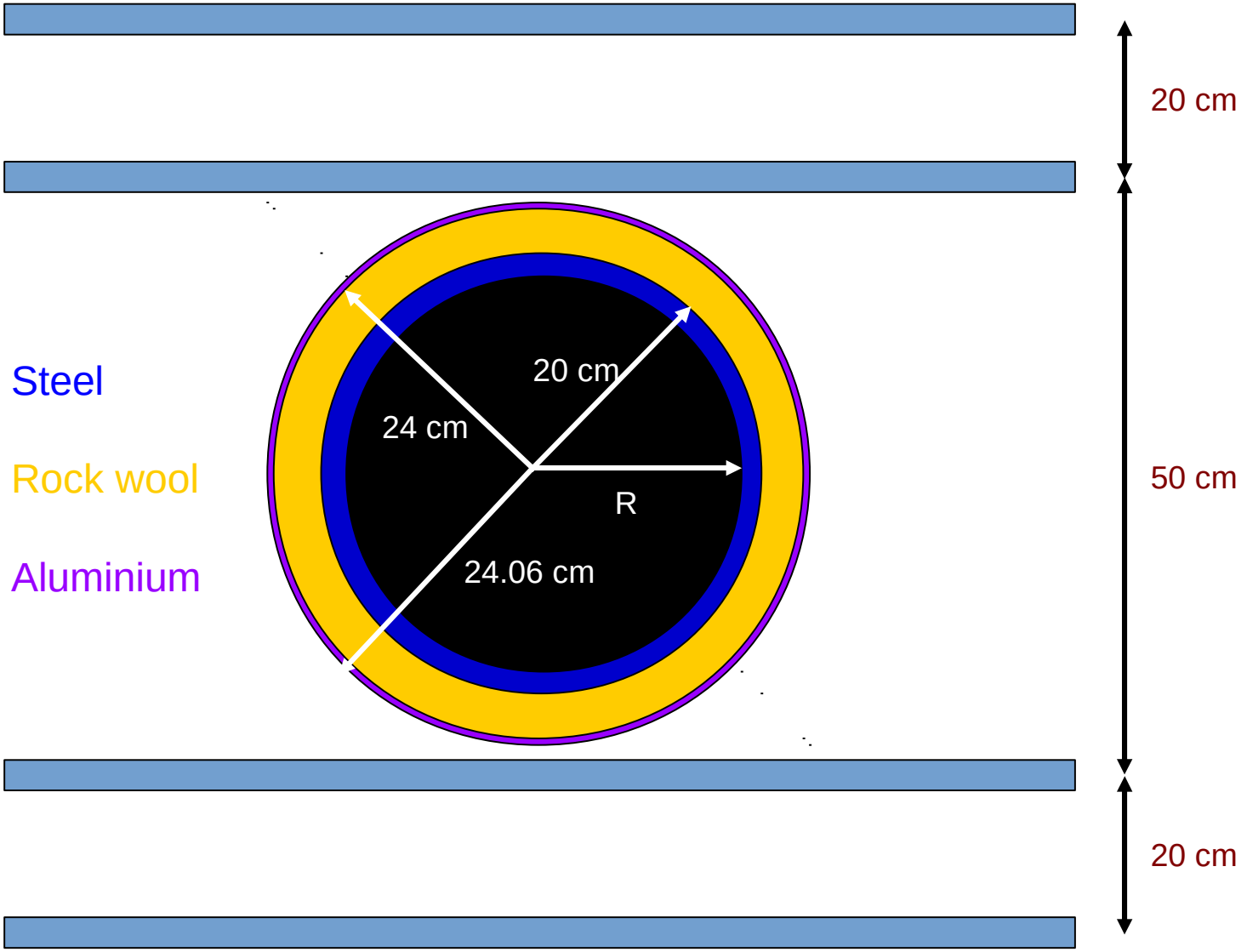

DOI:10.1098/rsta.2018.0054

Dynasol

Measurement of the width of an insulated pipe.

- Measure multiple scattering between the upper and lower trajectories.
- **Point of Closest Approach** → most likely scattering center.

Simulation Details:

CRY (*) generator.

Geant4 + local chamber response.

Assuming perfect resolution.

About 1 hour of data taking.

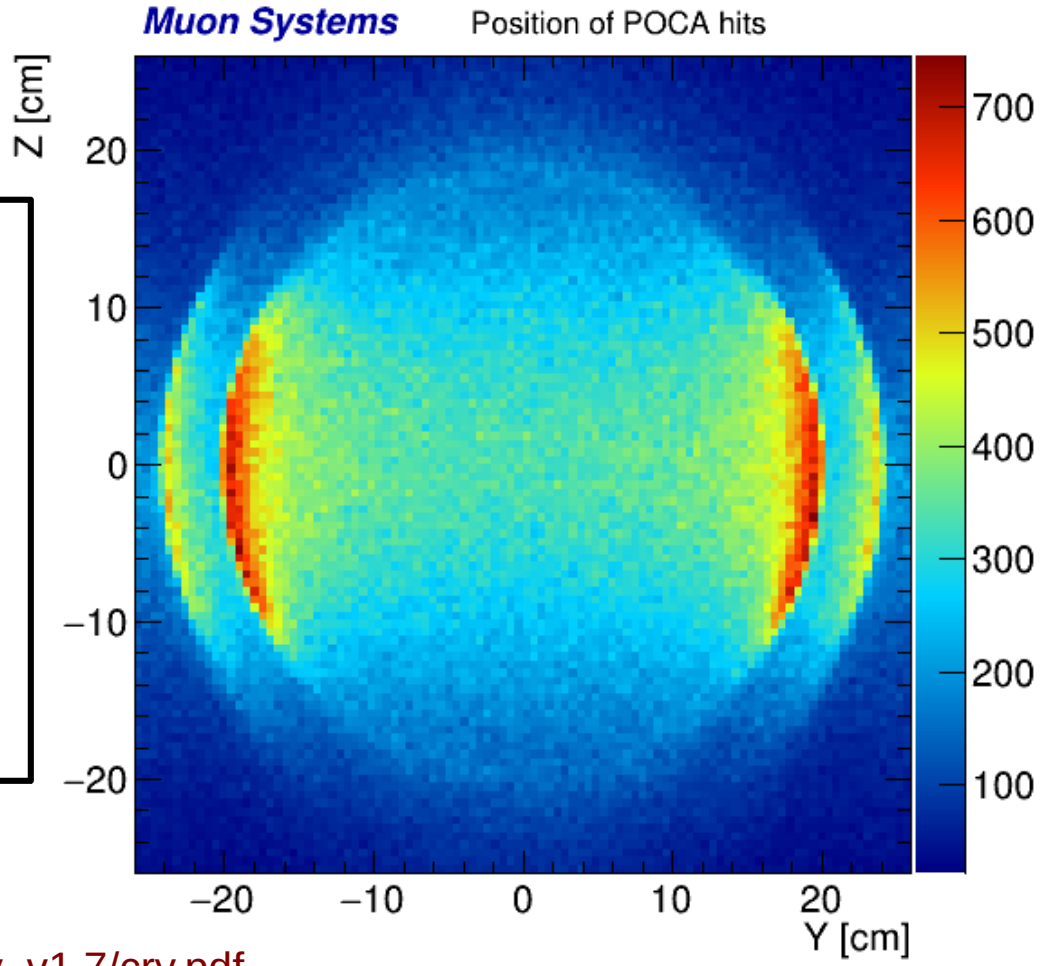

https://nuclear.llnl.gov/simulation/doc_cry_v1.7/cry.pdf

Reconstructed images for different widths.

Thickness = 1.2 cm

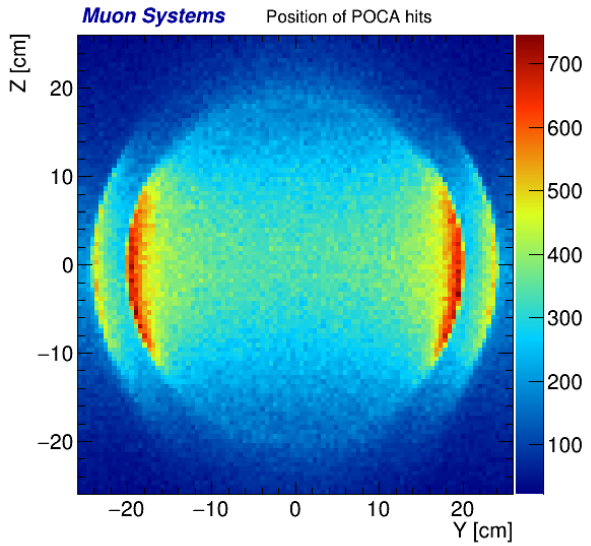

Thickness = 1.6 cm

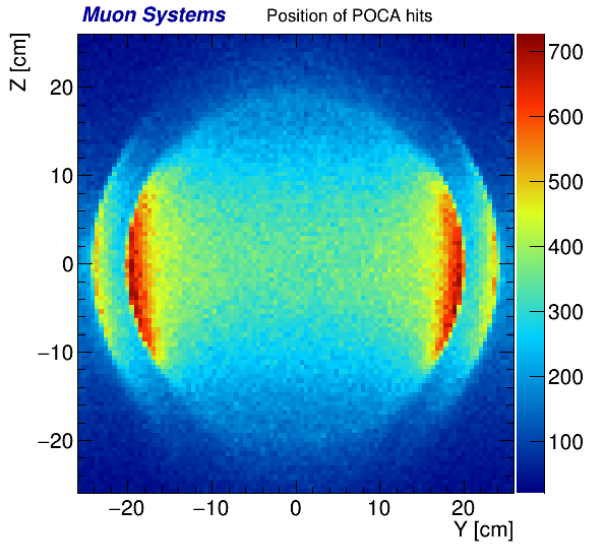

Thickness = 1.8 cm

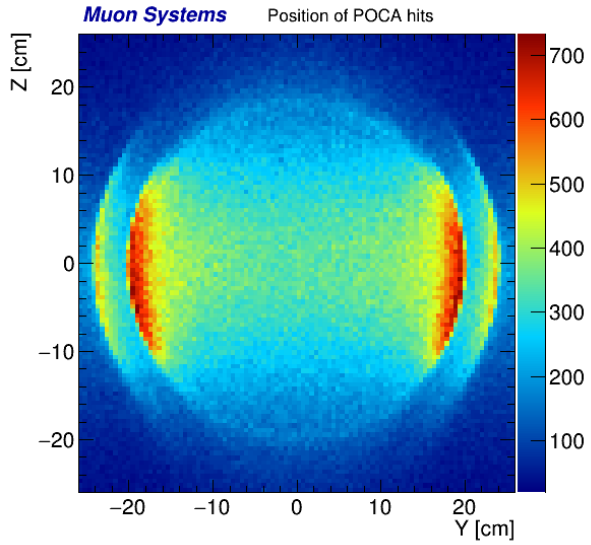

Thickness = 2.0 cm

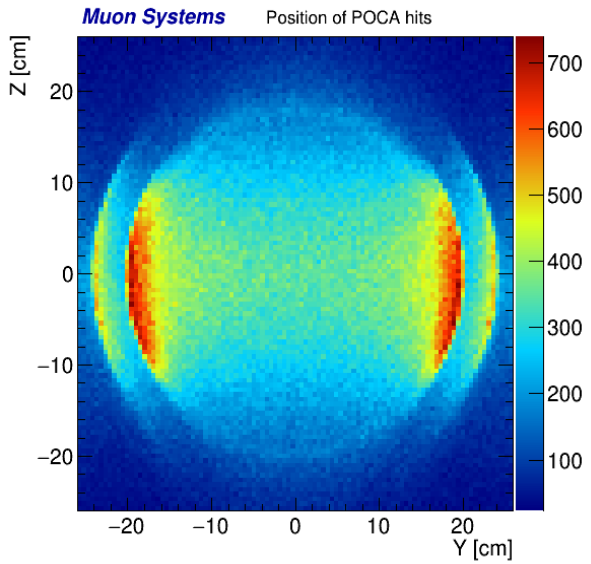

Thickness = 2.4 cm

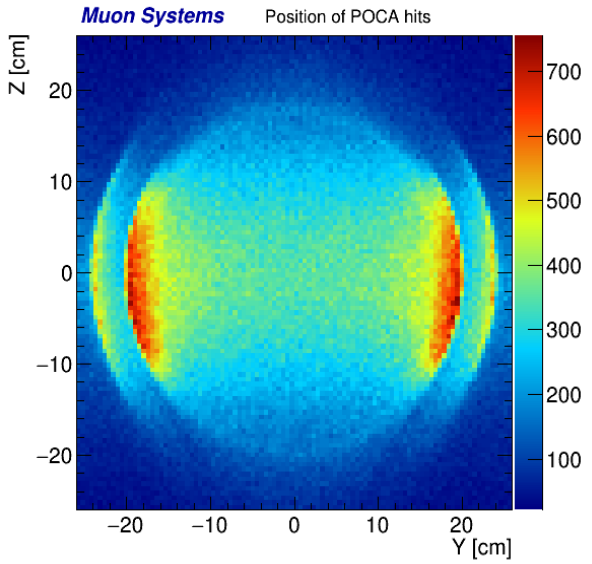

Thickness = 2.6 cm

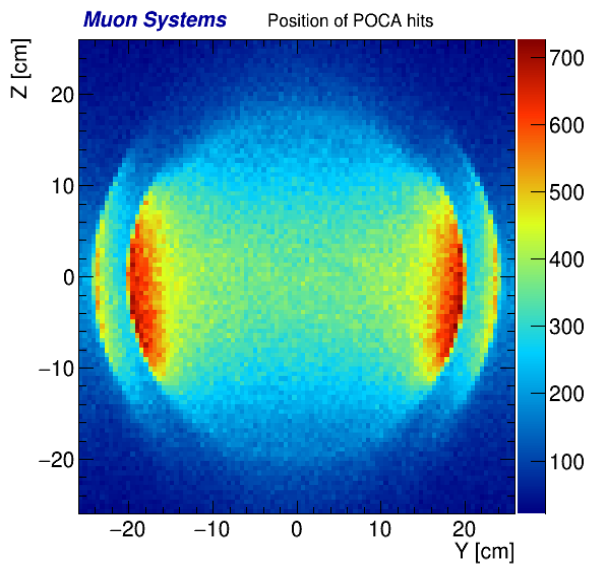

Simulations with realistic detector (4mm resolution)

- The loss of resolution makes it impossible to see the insulation layer.
- The steel wall is dense enough to be detected without problems.

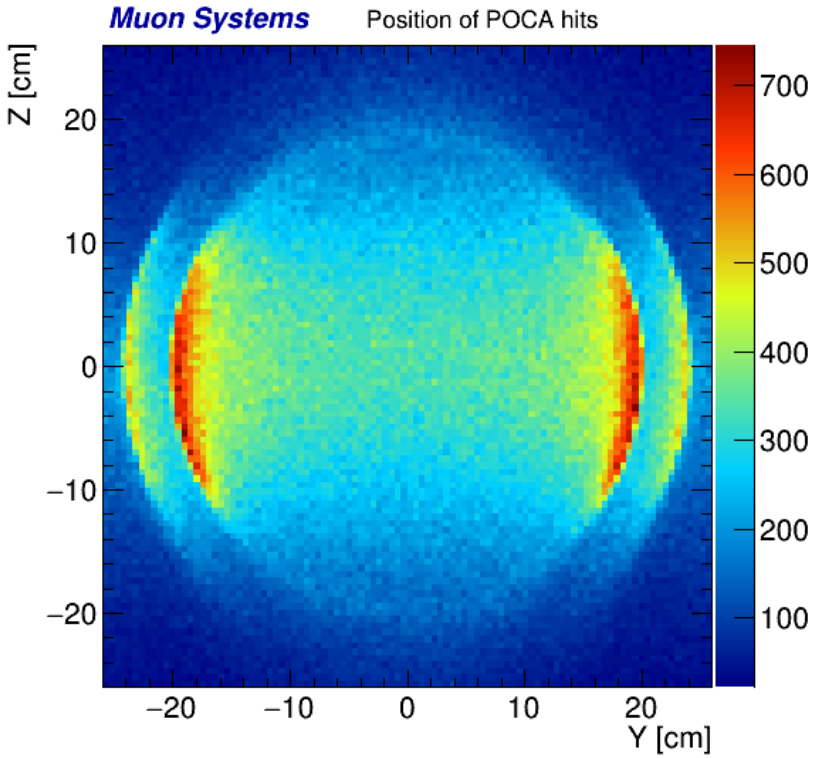

Perfect resolution

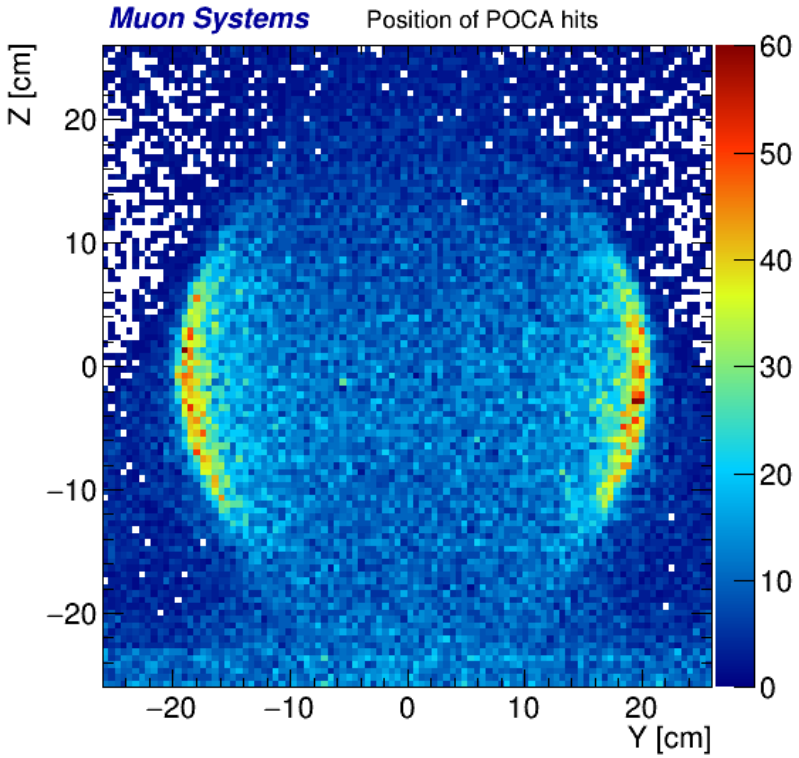

4 mm resolution

Simulations with realistic detector (4mm resolution)

Thickness = 1.2 cm

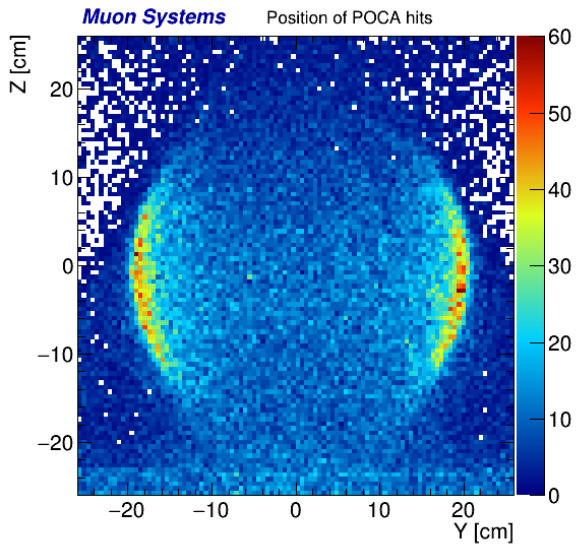

Thickness = 1.6 cm

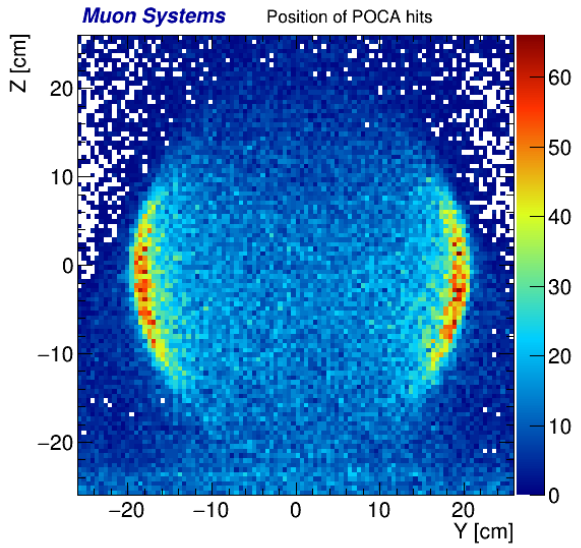

Thickness = 1.8 cm

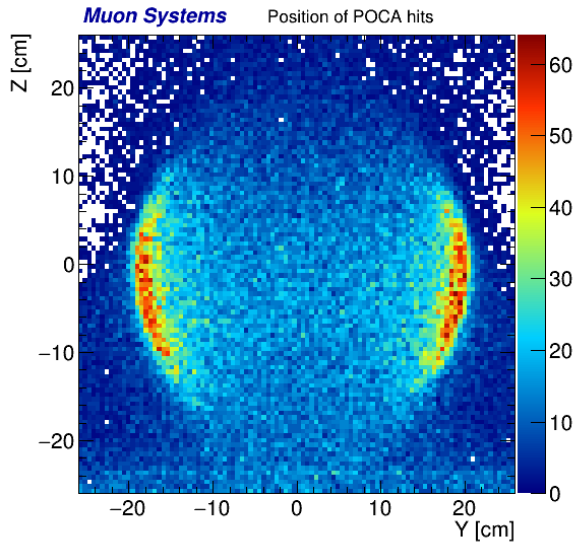

Thickness = 2.0 cm

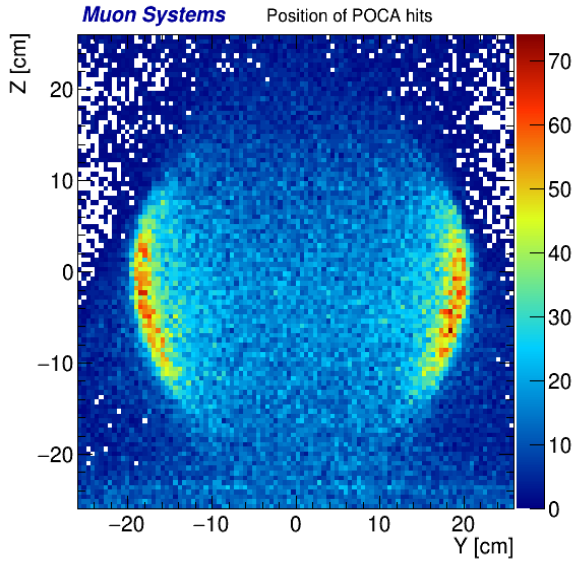

Thickness = 2.4 cm

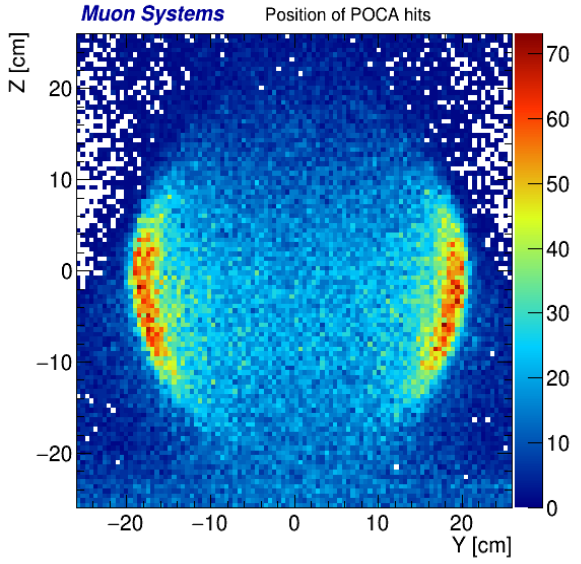

Thickness = 2.6 cm

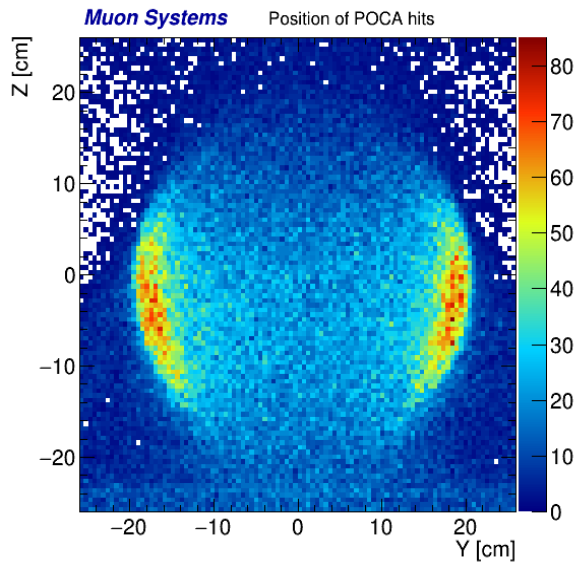

Simulations with realistic detector (4mm resolution)

- The loss of resolution makes it impossible to see the insulation layer.
- The differences in the radial distribution for the steel are still significant.
- **Algorithm** (*) looking for statistical compatibility between target and template.
- Reach resolutions of about 1-2 mm with 1 hour measurement.

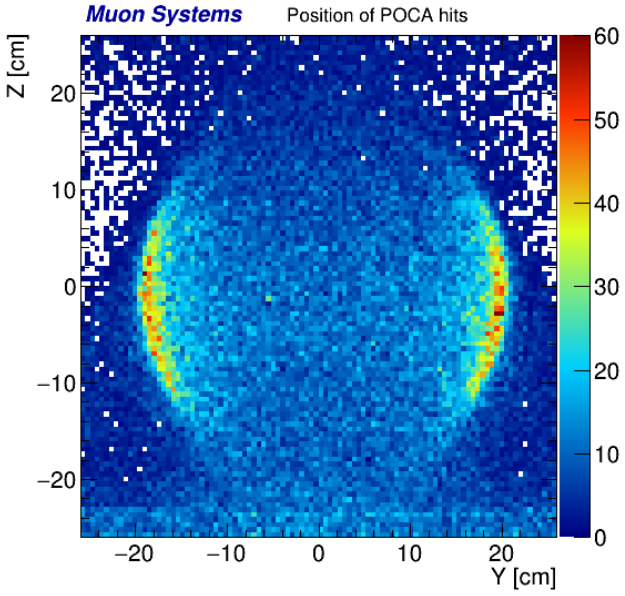

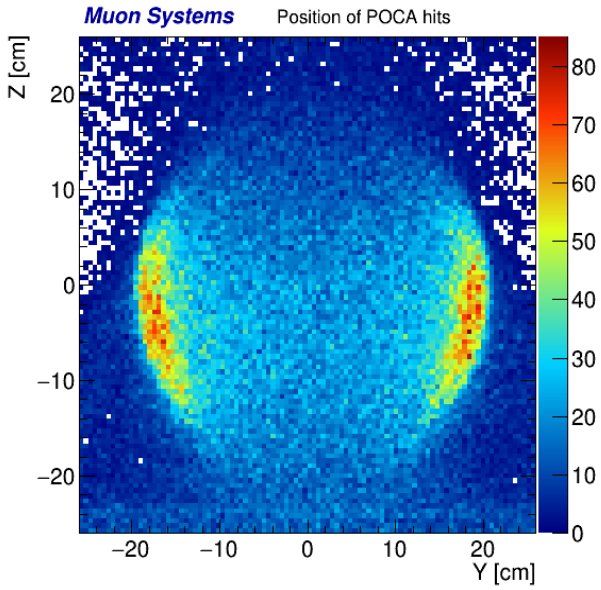

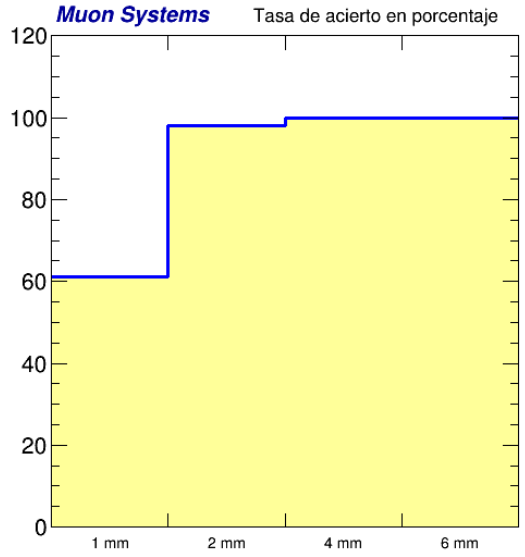

Accuracy

(*) Based on **Deep Learning Convolutional Network** no restricted to azymuthal asymmetry.

First prototype of (small) muon chambers.

Design with strips and multiplexing to save electronics.

ArCO2 gas

Gold-Tungsten wires

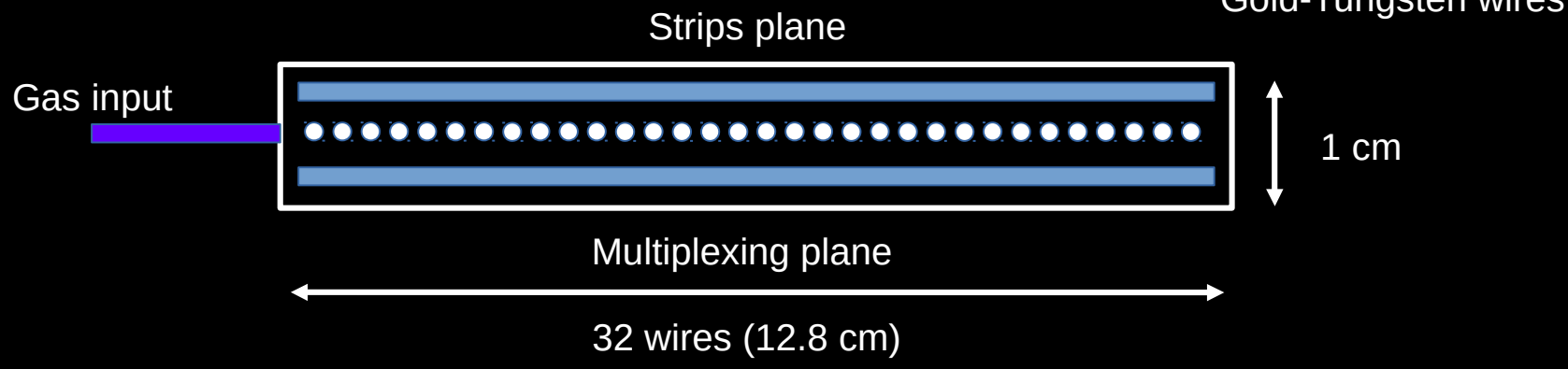

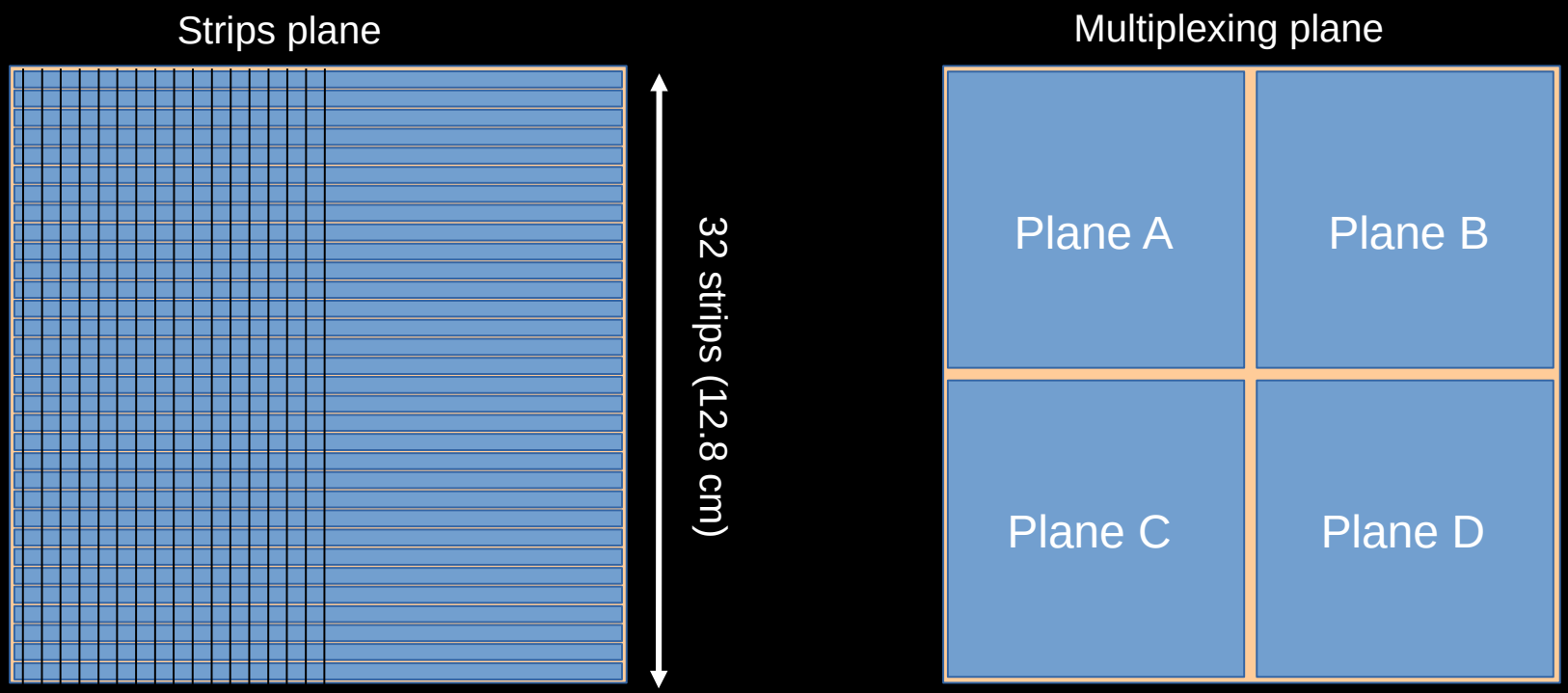

First prototype of (small) muon chambers.

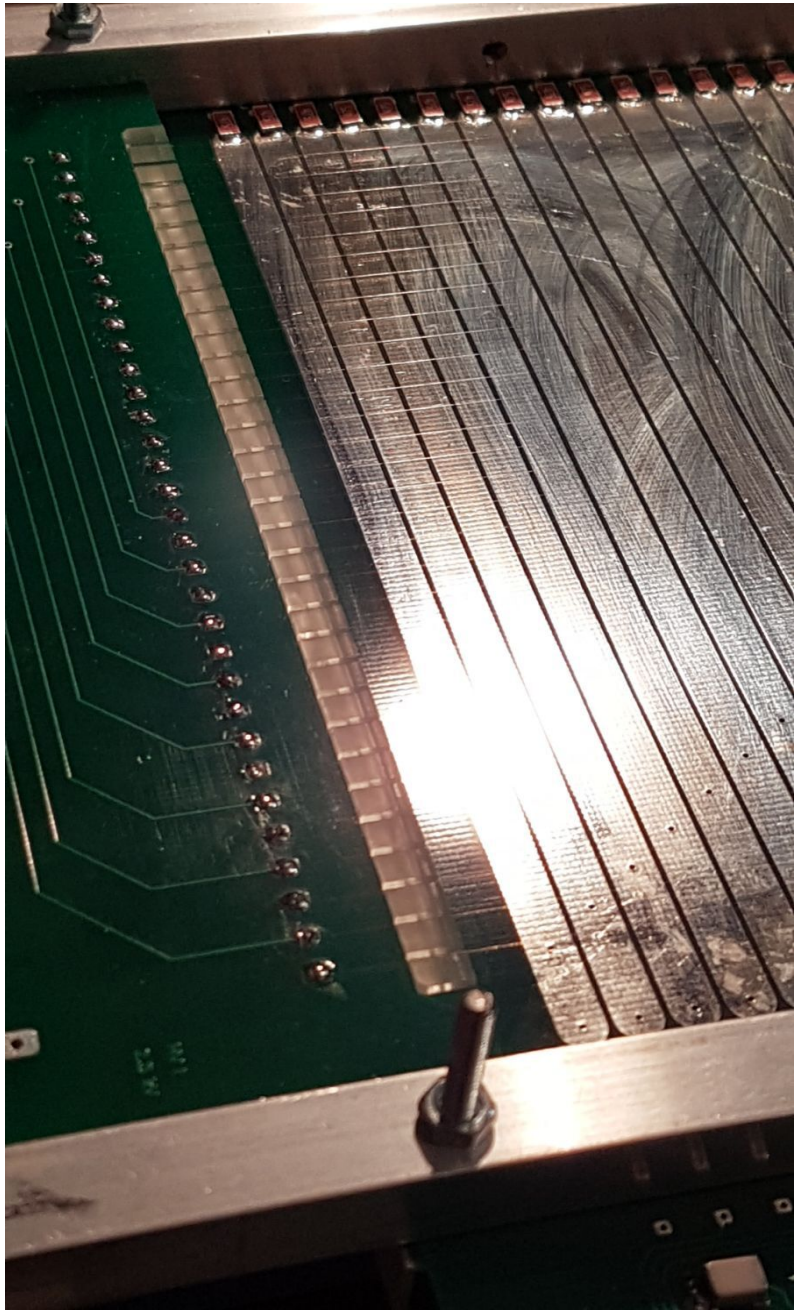

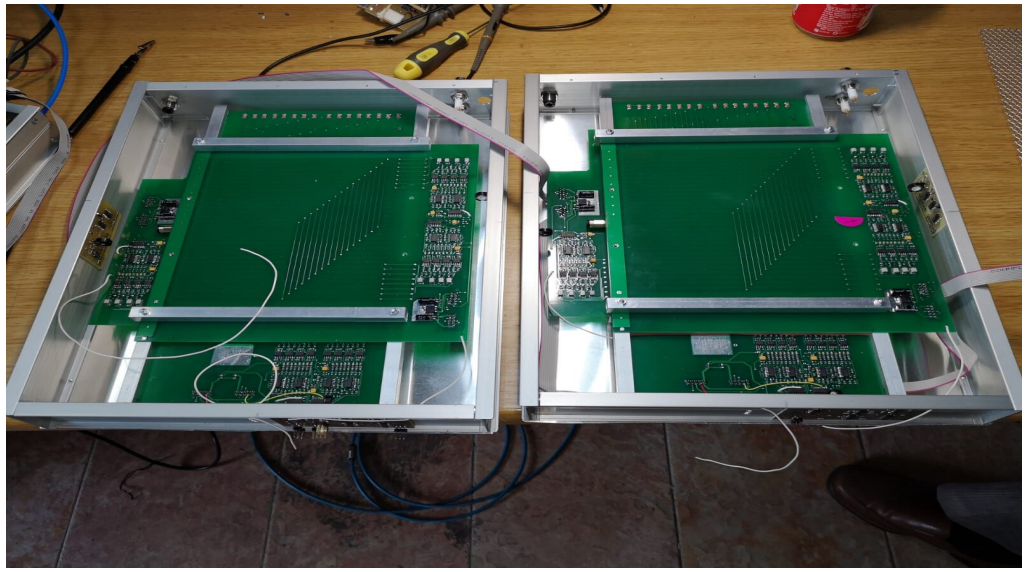

Simulations with realistic detector (4mm resolution)

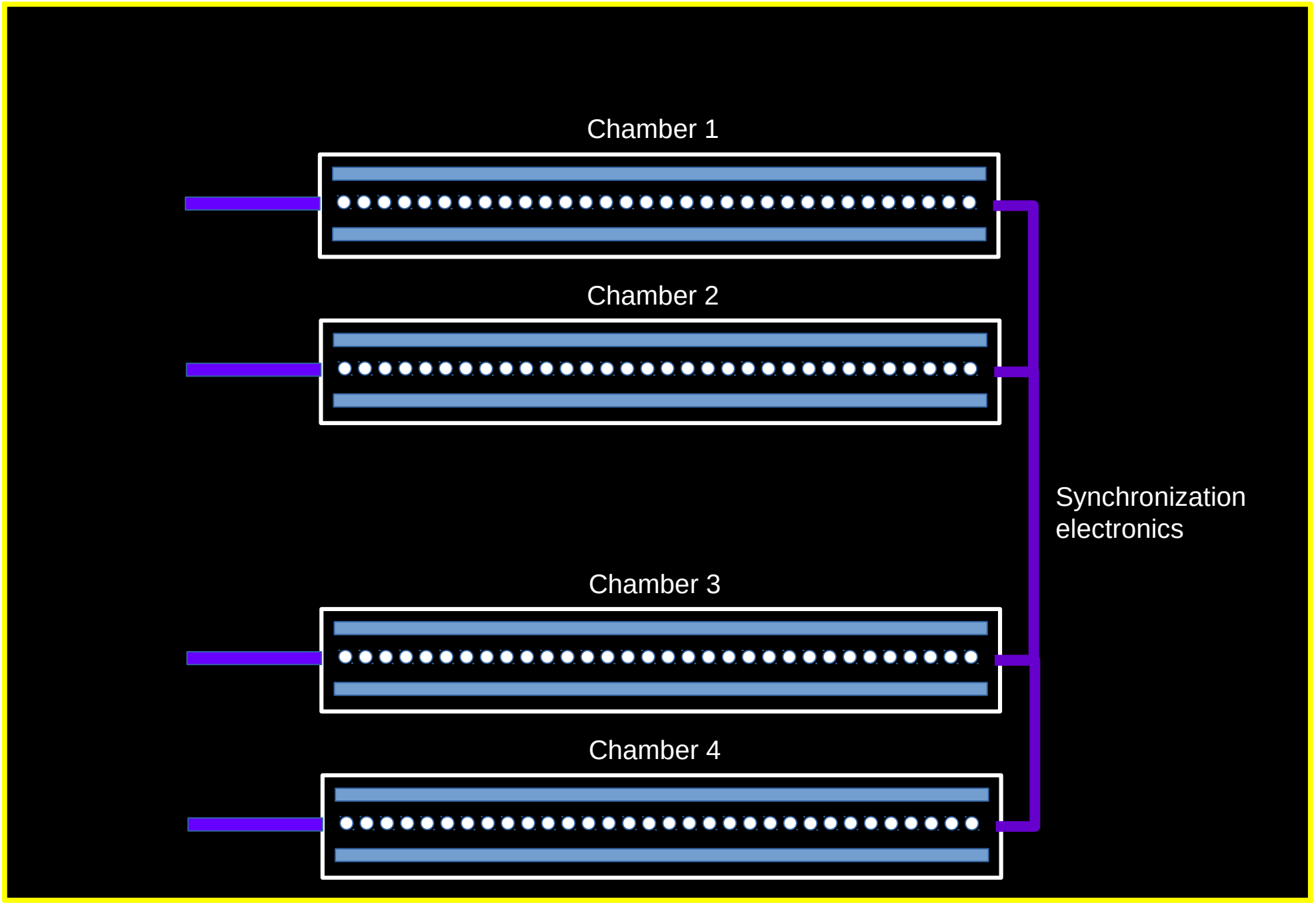

Commissioning of chambers (I).

Light DAQ and DQM running on Raspberry-Pi and sending data through wireless.

Good general functioning of individual chambers for wires.

Still low detection efficiency (~60%) due to multiplexing and strips.

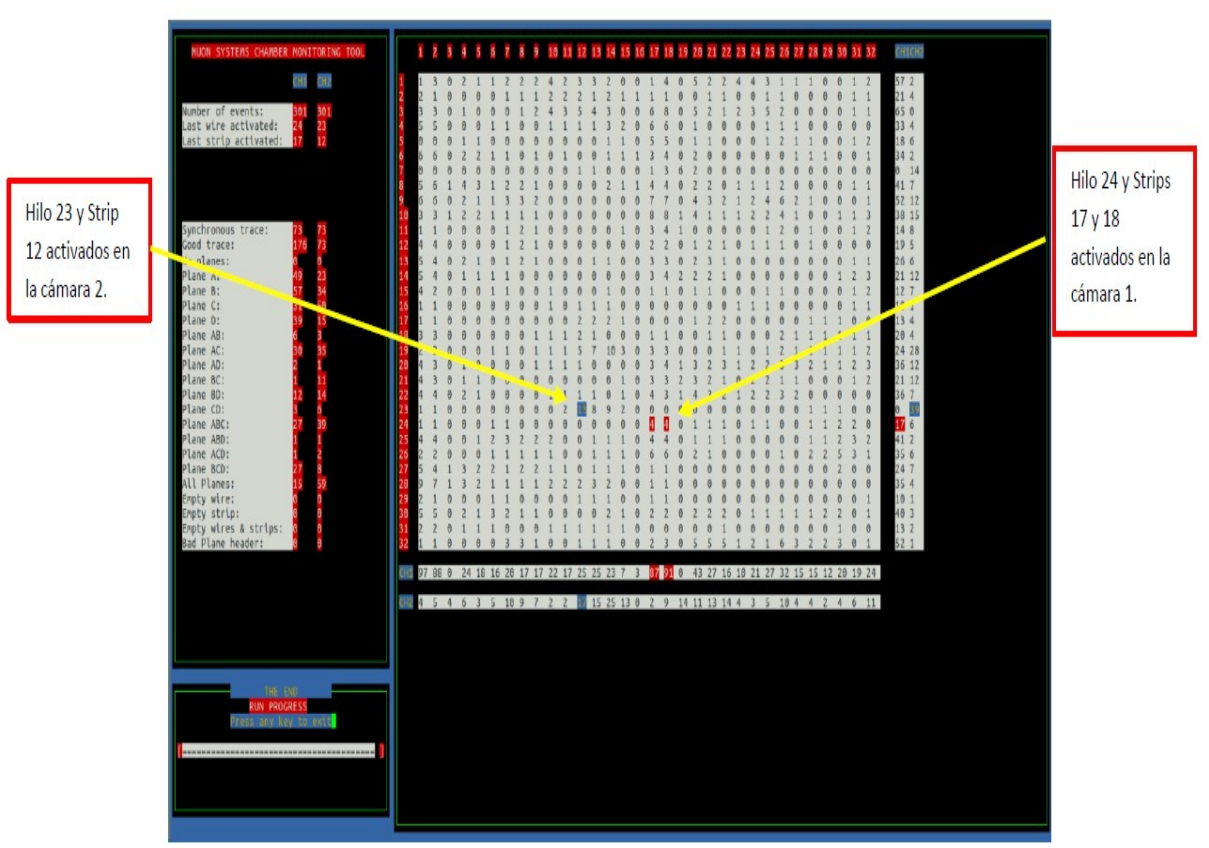

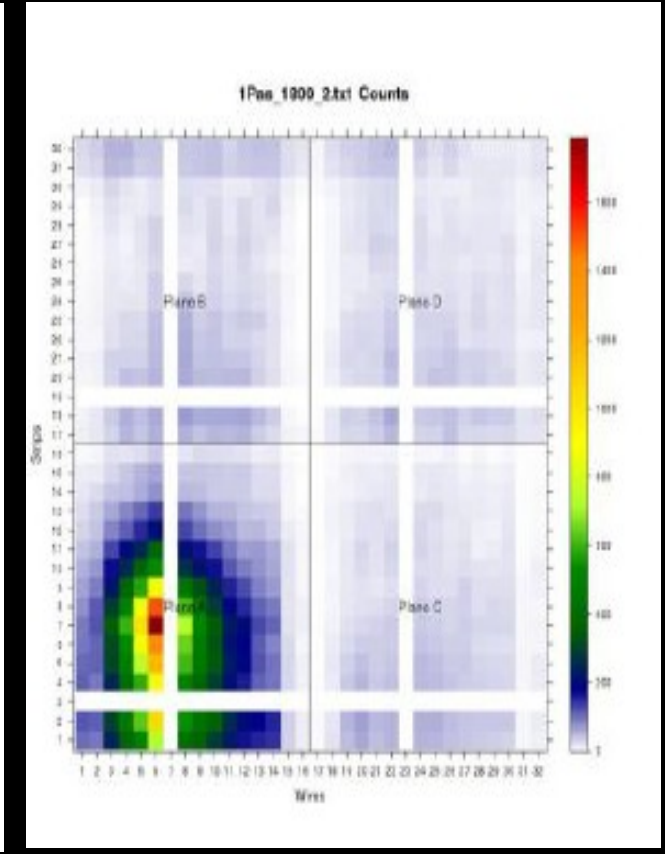

Commissioning of chambers (II).

First tracks reconstructed successfully with a high trigger efficiency (>95%)

Low detection efficiency in the strips coordinate (accumulated from individual chamber).

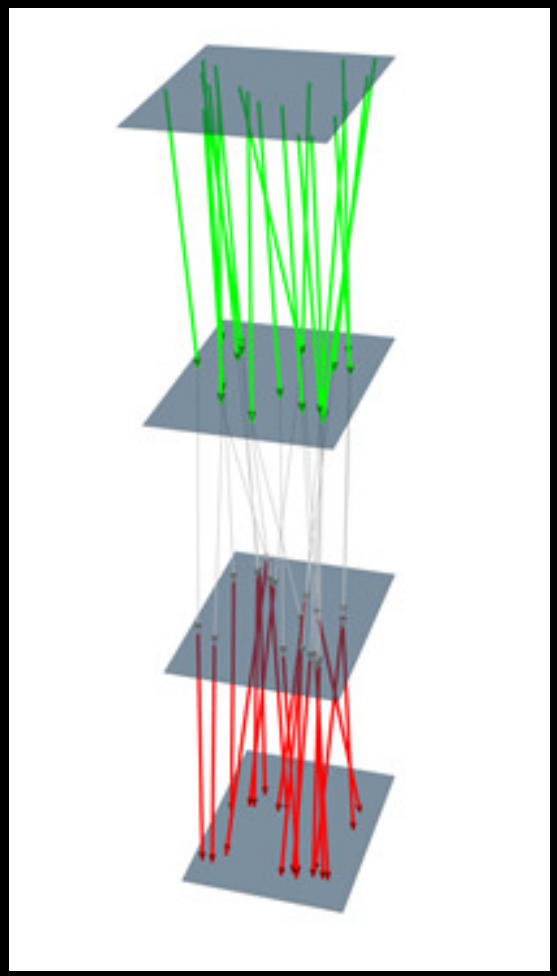

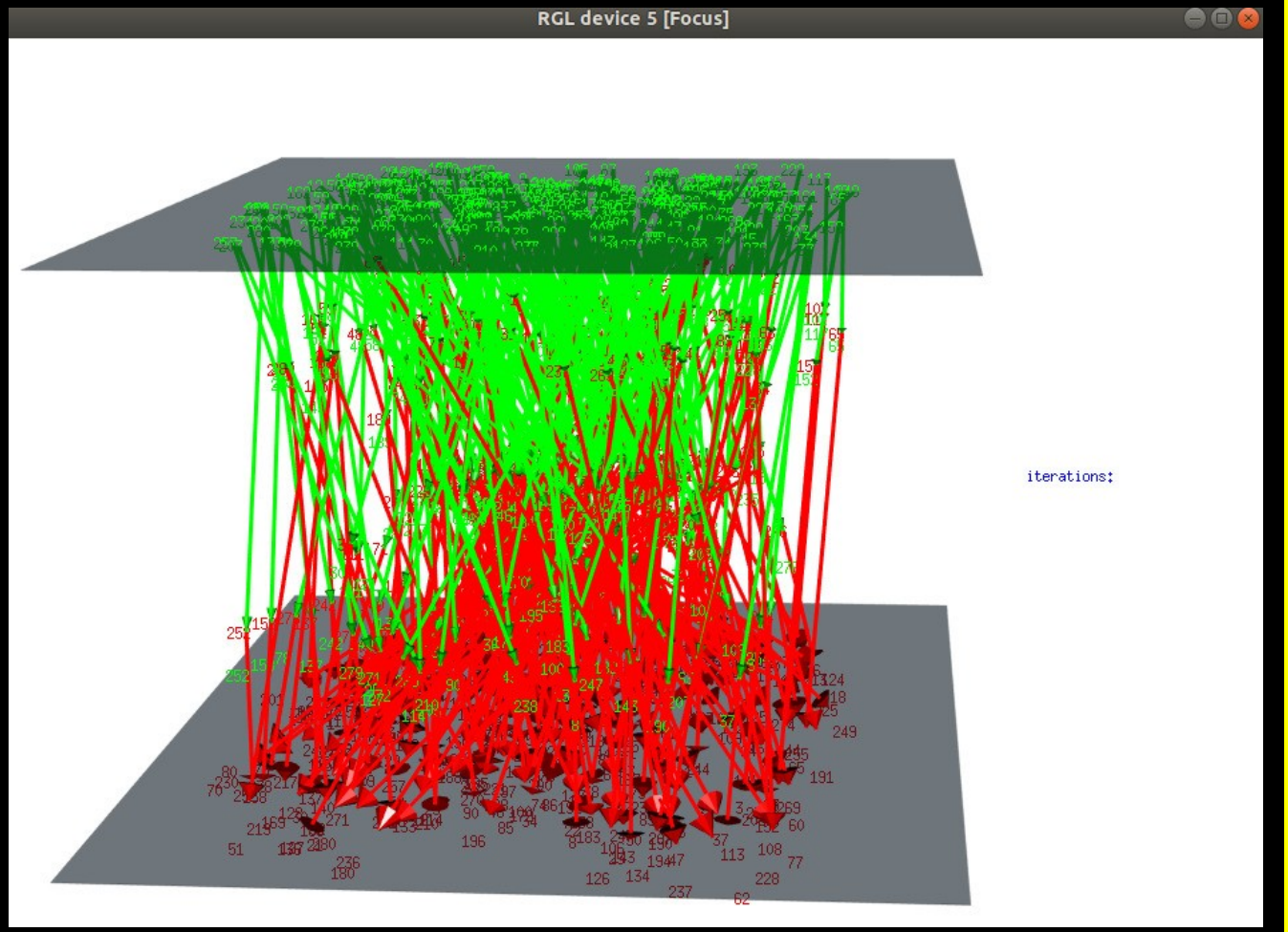

Detection of a 16 mm lead layer.

- Good agreement between data and simulation.
- Also good discrimination between the two scenarios.

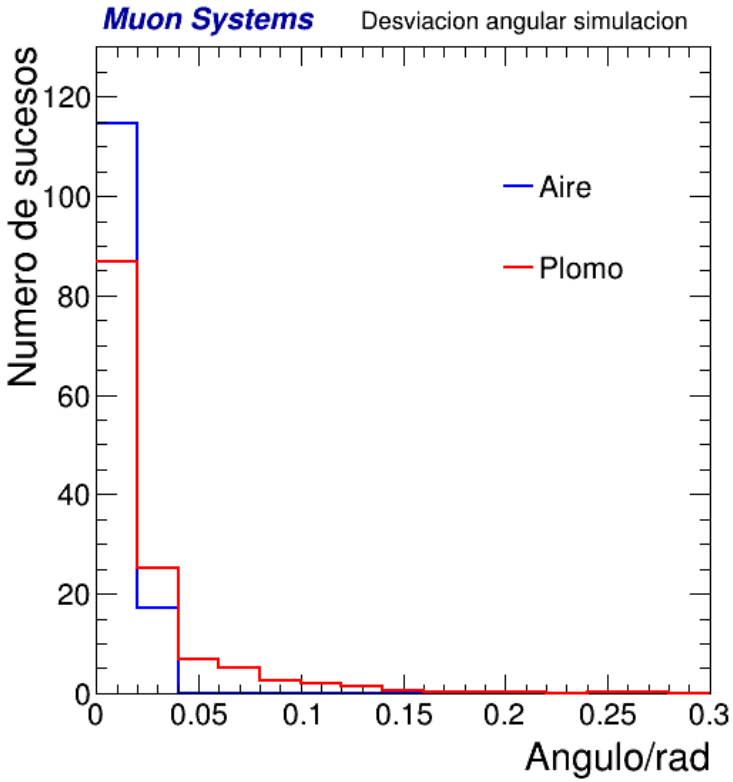

Simulation

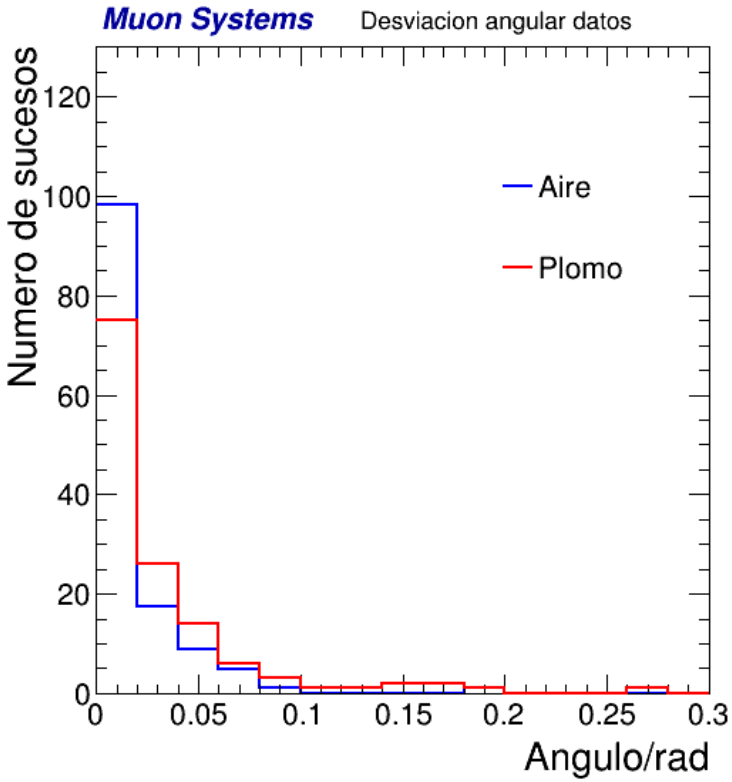

Real data

Lessons learned from 1st prototype.

- Good functioning and response of the wires → high efficiency system.
- Strips discarded because of multiple strip activation per event.
- Good functioning of electronics and trigger system (very high efficiency).
- Need to scale the system to increase the acceptance.

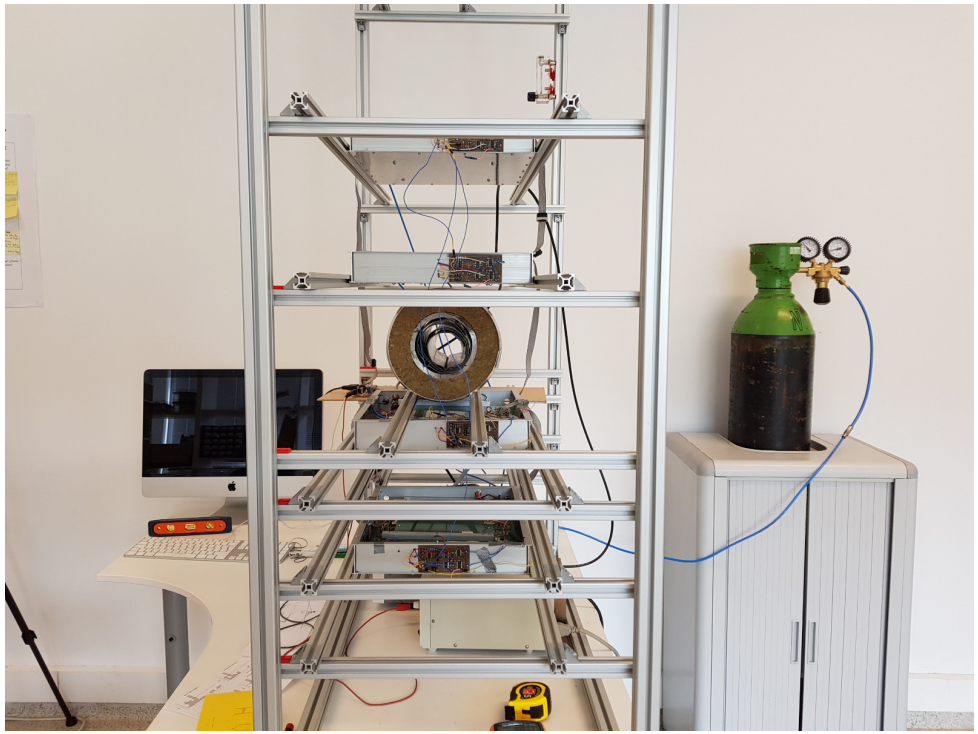

The future of muography and next steps.

Scaling detectors to 1 squared meter dimension.

Improving reconstruction algorithms (I)

- Consider the quartiles of distributions of the following parameters as input to DNN
  - Entrance position and direction of the muon. (x, y)
  - Deviation in position and direction as measured by second muon. (x,y)
  - Products of these variables.
- Consider the density of every voxel as the output of the DNN.

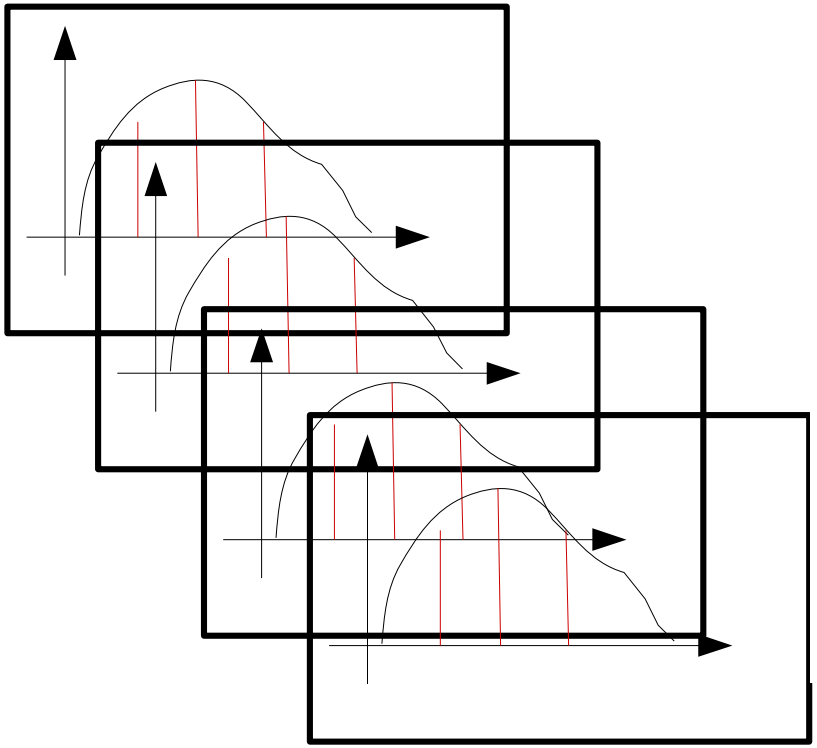

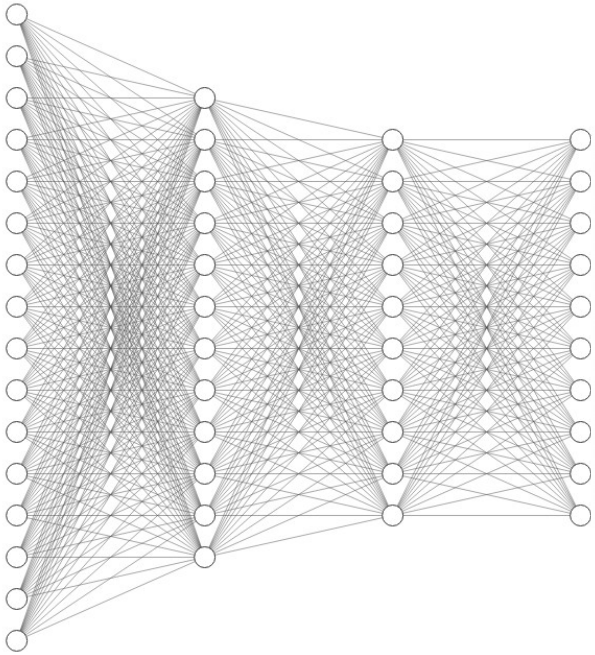

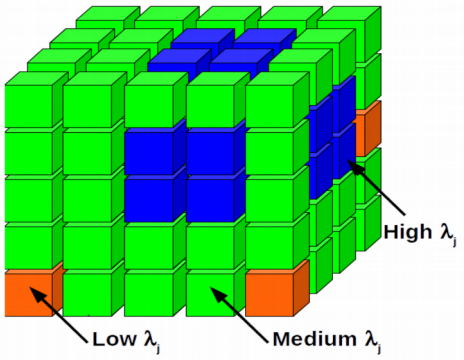

Improving reconstruction algorithms (II)

- Map positions and directions in the detectors to integers.

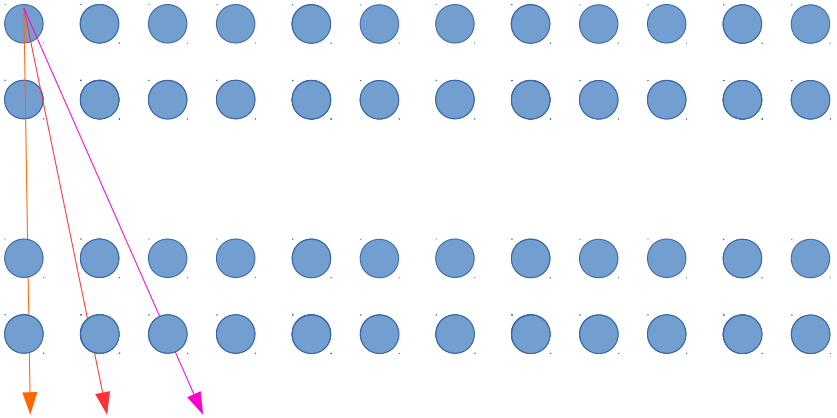

N = {1, 2, 3,...}

- In this way all possible tracks are indexed and the input and output are encoded.
- The number of events found on each index is fed as the input of the DNN.
- The output is the density per voxel in the output geometry.

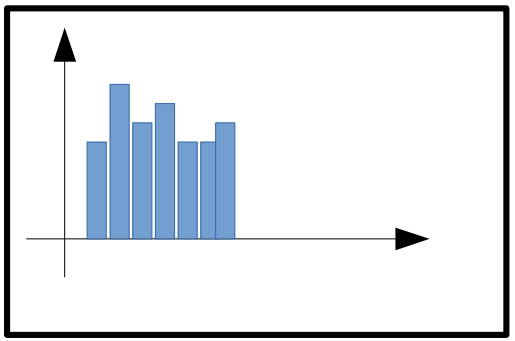

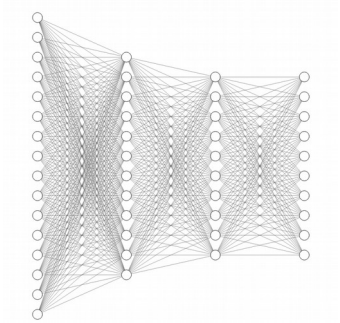

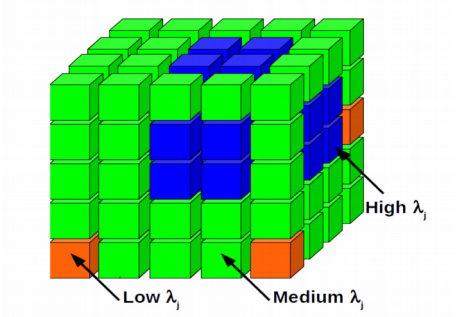

Next steps for Muon Systems.

- Detector construction will be ready in the next months.
- Expect to perform commissioning in the lab before the Summer.
- Plan to do an on-site pilot test in Dynasol in Santander to measure Pipes.

Dynasol

International consortium of Muographers.

- Muography is slowly entering into a commercial phase.
- Attempts hosted by the **IAEA** and the **Royal Society** to create a consortium.
  - Idea is to work together to promote the technology worldwide.

THANK YOU

Muon Tomography Systems SL
www.muon.systems
Av. Altos Hornos de Vizcaya 33
48901 Barakaldo (Bizkaia)